Metabolism 146 (2023) 155661

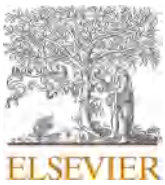

Contents lists available at ScienceDirect

Metabolism

journal homepage: www.journals.elsevier.com/metabolism

Hepatocyte-secreted FAM3D ameliorates hepatic steatosis by activating FPR1-hnRNP U-GR-SCAD pathway to enhance lipid oxidation

Yuntao Hu [a,1], Jing Li [b,1], Xin Li [a], Di Wang [c], Rui Xiang [a], Wenjun Liu [a], Song Hou [a], Qinghe Zhao [d], Xiaoxing Yu [a], Ming Xu [e], Dong Zhao [f], Tao Li [g], Yujing Chi [c,d,*], Jichun Yang [a,h,*]

[a] Department of Physiology and Pathophysiology, School of Basic Medical Sciences, State Key Laboratory of Vascular Homeostasis and Remodeling, Center for Non-coding RNA Medicine, Peking University Health Science Center, Beijing 100191, China
[b] Department of Endocrinology, Beijing Chao-Yang Hospital, Capital Medical University, Beijing 100027, China
[c] Department of Central Laboratory and Institute of Clinical Molecular Biology, Peking University People's Hospital, Beijing 100044, China
[d] Department of Gastroenterology, Peking University People's Hospital, Beijing 100044, China
[e] Department of Cardiology, Institute of Vascular Medicine, Peking University Third Hospital, Key Laboratory of Molecular Cardiovascular Science of the Ministry of Education, Beijing 100191, China
[f] Department of Endocrinology, Beijing Luhe Hospital, Capital Medical University, Beijing 101100, China
[g] Department of Hepatobiliary Surgery, Peking University People's Hospital, Beijing 100044, China
[h] Department of Cardiology, Peking University Third Hospital, Beijing 100191, China

ARTICLE INFO

Keywords:
Family with sequence similarity 3
Member D
Formyl peptide receptor 1
Short-chain acyl-CoA dehydrogenase
Lipid oxidation
Glucocorticoid receptor

ABSTRACT

Nonalcoholic fatty liver disease (NAFLD) is the most common chronic liver disease worldwide; however, the underlying mechanisms remain poorly understood. FAM3D is a member of the FAM3 family; however, its role in hepatic glycolipid metabolism remains unknown. Serum FAM3D levels are positively correlated with fasting blood glucose levels in patients with diabetes. Hepatocytes express and secrete FAM3D, and its expression is increased in steatotic human and mouse livers. Hepatic FAM3D overexpression ameliorated hyperglycemia and steatosis in obese mice, whereas FAM3D-deficient mice exhibited exaggerated hyperglycemia and steatosis after high-fat diet (HFD)-feeding. In cultured hepatocytes, FAM3D overexpression or recombinant FAM3D protein (rFAM3D) treatment reduced gluconeogenesis and lipid deposition, which were blocked by anti-FAM3D antibodies or inhibition of its receptor, formyl peptide receptor 1 (FPR1). FPR1 overexpression suppressed gluconeogenesis and reduced lipid deposition in wild hepatocytes but not in FAM3D-deficient hepatocytes. The addition of rFAM3D restored FPR1's inhibitory effects on gluconeogenesis and lipid deposition in FAM3D-deficient hepatocytes. Hepatic FPR1 overexpression ameliorated hyperglycemia and steatosis in obese mice. RNA sequencing and DNA pull-down revealed that the FAM3D-FPR1 axis upregulated the expression of heterogeneous nuclear ribonucleoprotein U (hnRNP U), which recruits the glucocorticoid receptor (GR) to the promoter region of the short-chain acyl-CoA dehydrogenase (SCAD) gene, promoting its transcription to enhance lipid oxidation. Moreover, FAM3D-FPR1 axis also activates calmodulin-Akt pathway to suppress gluconeogenesis in hepatocytes. In conclusion, hepatocyte-secreted FAM3D activated the FPR1-hnRNP U-GR-SCAD pathway to enhance lipid oxidation in hepatocytes. Under obesity conditions, increased hepatic FAM3D expression is a compensatory mechanism against dysregulated glucose and lipid metabolism.

1. Introduction

Nonalcoholic fatty liver disease (NAFLD) has emerged as the most common form of chronic liver disease [1]. Over the past decade, the prevalence and incidence of NAFLD have increased worldwide [2]. A recent study revealed that the highest prevalence of NAFLD was in Latin America (44.37 %), followed by the Middle East and North Africa (36.53 %), South Asia (33.83 %), Southeast Asia (33.07 %), North America (31.20 %, 25.86 %–37.08 %), East Asia (29.71 %), Asia-Pacific (28.02 %), and Western Europe (25.10 %) [3]. It has been estimated that

* Corresponding authors.
E-mail addresses: chiyujing@bjmu.edu.cn (Y. Chi), yangj@bjmu.edu.cn (J. Yang).
[1] These authors contributed equally.

https://doi.org/10.1016/j.metabol.2023.155661
Received 29 April 2023; Accepted 11 July 2023
Available online 16 July 2023

NAFLD could increase the prevalence and economic burden of end-stage liver disease by 2–3-fold in Western countries and several Asian countries by 2030 [4]. NAFLD is a hepatic manifestation of systemic metabolic disorders and is closely associated with metabolic syndrome [4–6]. Considering the complexity of the metabolic regulatory network in the liver, it is necessary to identify novel and important regulators of hepatic glucose and lipid metabolism.

The family with sequence similarity 3 (FAM3) is a cytokine-like gene family consisting of four members designated as FAM3A, FAM3B, FAM3C, and FAM3D, respectively [7]. To date, we and others have demonstrated that FAM3A, FAM3B, and FAM3C play crucial roles in the regulation of glucose and lipid metabolism in the liver and other tissues [7]. The dysregulated expression and signal transduction of FAM3A, FAM3B, and FAM3C are widely involved in the pathogenesis of metabolic diseases [8–10]. As a mitochondrial protein, FAM3A interacts with F1-ATP synthase (ATPS) and regulates the expression of the transcription factor forkhead box protein D3 (FOXD3) to regulate the activity and assembly of ATPS, thereby controlling ATP production [11]. The released ATP activates the P2 receptor-Ca^{2+}-CaM-PI3K-Akt pathway to suppress hepatic gluconeogenesis independent of insulin [9]. FAM3A also activates the ATP-P2 receptor-CaM-FOXA2-CPT2 pathway to promote lipid oxidation in the liver and the ATP-CaM-FOXA2-UCP2 pathway to increase thermogenesis in brown adipose tissues [12]. FAM3B acts as a co-activator of FOXO1 to promote hepatic gluconeogenesis and lipogenesis [8,13]. FAM3C activates the HSF1-CaM-Akt pathway to ameliorate hyperglycemia and fatty liver, independent of insulin [10]. Identification of the regulatory network of the FAM3 gene family, particularly the insulin-independent FAM3A and FAM3C metabolic pathways in the liver, has greatly expanded our understanding of the pathogenesis of metabolic diseases and provides viable targets for developing novel strategies to treat them [8–12,14].

FAM3D, also known as oncoprotein-induced transcript 1 (Oit1) in mice, is highly expressed in the gastrointestinal tract of humans and mice [15]. Further studies have confirmed that FAM3D is specifically expressed in the mouse colon and human small intestine, and plays a critical role in maintaining colon homeostasis [16]. As a secretory protein, FAM3D is secreted from intestinal epithelial cells into the lumen and/or basolateral sites, enters blood circulation, and acts on different tissues and organs [15,17]. Plasma FAM3D levels vary with nutritional status [15,18]. Human serum FAM3D levels were significantly higher after consuming high-fat diets for 4h than after consuming a low-fat diet [15]. FAM3D can induce mitogen-activated protein kinase phosphatase 1 (MKP1) to inhibit the phosphorylation of extracellular regulated protein kinases (ERK) and suppress the activation of prohormone convertase 2 (PC2) to inhibit glucagon secretion in pancreatic islet alpha cells [19]. Although several lines of evidence suggest that FAM3D plays an important role in regulating glucose and lipid metabolism, further studies are needed to verify this.

Cytokines exert their biological functions primarily through their receptors. Formyl peptide receptors (FPRs) are a class of G-protein-coupled receptors (GPCRs) with seven transmembrane domains [20]. The FPRs family is mainly composed of formyl peptide receptor 1 (FPR1), FPR2, and FPR3, which play important defensive and anti-inflammatory roles in cells [21]. The expression profiles of FPR1 and FPR2 are similar, and both are expressed in mouse abdominal neutrophils [21]. FPR3 transcript was not found in neutrophils but was detected in monocytes [21]. Peng et al. first found that FAM3D is an endogenous agonist of FPR1/2 and has a strong chemotactic effect on polymorphonuclear neutrophils (PMNs) and peripheral blood mononuclear cells (PBMs) isolated from human peripheral blood; further mechanical studies confirmed that FPR1 and FPR2 are FAM3D receptors [22]. Another study revealed that FAM3D promotes neutrophilic recruitment through FPR1 to exacerbate the development of abdominal aortic aneurysms (AAA) [23]. However, the role of FPR1 in regulating glucose and lipid metabolism remains poorly understood. In pancreatic islet alpha cells, FAM3D inhibits glucagon secretion and PC2 activity via FPR2 [19]. Previous studies have shown that FPR1-mediated N-formyl-Met-Leu-Phe (fMLF) induces Ca^{2+} mobilization in a pertussis toxin (PTX)-dependent manner [24] and that FAM3D enhances FPR1- or FPR2-mediated Ca^{2+} influx in HEK293 cells [22].

The current study aimed to determine the role and mechanism of FAM3D and its receptor, FPR1, in the regulation of hepatic glucose and lipid metabolism.

2. Materials and methods

2.1. Clinical samples

The plasma of healthy individuals and patients with diabetes used in this study had obtained the healthy individuals' and patients' informed consent and had been approved by the Ethics Committee of Beijing Luhe Hospital (Ethics Number 2016YFC0901200). The physiological and biological parameters are detailed in Supplemental Table 1. The clinical liver histopathology specimens used in this study were obtained from surgical resections of patients with non-neoplastic liver diseases. All diagnoses of NAFLD were based on histopathological examinations. The human tissue samples used in this study were in accordance with the ethical approval of the Research Ethics Committee of Peking University People's Hospital (Ethics Number 2020PHB337–01), and the clinical characteristics of these human subjects are detailed in Supplemental Table 2.

2.2. Animals

8 to 10-week-old male C57BL/6 J and FAM3D$^{-/-}$ mice with C57BL/6 J background and 8 to 12-week-old male db/db mice on BKS background were used in this study. FAM3D$^{-/-}$ mice were generated on a C57BL/6 J background by TALEN technology, and kindly gifted by Prof. Kong (School of Basic Medical Sciences, Peking University), as detailed in the previous study [23]. The T7E1 assay (Viewsolid Biotech, Beijing, CN) and sequence analysis (Sunbio, Beijing, CN) were used for genotyping identification. Wild-type (WT) or FAM3D$^{-/-}$ mice were fed on a 45 % high-fat diet (HFD, MD12032, Medicience, Jiangsu, CN) or normal diet (ND) for 12 weeks, respectively. Mice were fed in a controlled environment with a temperature of 22.5 ± 2.5 °C and a humidity of 55 ± 10 %, and housed in a standard 12-hour dark-light cycle with water and food ad libitum. All animal experiments were approved by the Institutional Animal Care and Use Committee of Peking University Health Science Center (LA2018179).

2.3. Overexpression of FAM3D or FPR1 in mouse livers

Homo FAM3D-overexpressing plasmid was kindly gifted by Prof. Kong [23] and then constructed by WZ Biosciences Inc. 1.5×10^9 pfu FAM3D-overexpressing adenovirus (Ad-FAM3D) or control adenovirus (Ad-GFP) were injected into the tail vein of C57BL/6 J mice or HFD mice after feeding on 45 % HFD for 12 weeks. The homo FPR1 expression plasmid was kindly provided by Prof. Kong [23] and then constructed into an adeno-associated virus 8 vector with the CMV promoter (aav-FPR1) (WZ Biosciences Inc., CN). db/db mice were injected with 5×10^{11} vg aav-FPR1 (aav-GFP as a control) via tail vein.

2.4. Primary mouse hepatocytes culture

8 to 10-week-old male C57BL/6 J mice were used to isolate primary hepatocytes as detailed previously [9].

2.5. OGTT/PTT/ITT

The detailed protocols for the oral glucose tolerance test (OGTT), insulin tolerance test (ITT), and pyruvate tolerance test (PTT) have been described in our previous studies [12].

2.6. Magnetic resonance imaging (MRI) analyses

Mice were placed horizontally in a sealed small-animal MRI mounting plate and continuously anesthetized with isoflurane (cat. no. W100). Fat distribution and images of the liver and body were collected and quantitatively analyzed using a Siemens MRI system 3.0 T, a Trio Tim scanner, and Siemens Syngo software Mr. B17, as previously described [12].

2.7. Metabolic cage analyses

Each mouse was housed individually in an environmentally controlled (22.5 ± 2.5 °C) sealed metabolic cage for 24 h to monitor energy expenditure (EE), respiratory exchange rate (RQ), physical activities, and food intake. RQ and EE were calculated using the Comprehensive Laboratory Animal Monitoring System formula, as previously described [12]. Physical activity was monitored using horizontal and vertical infrared sensor pairs arranged on the strips.

2.8. Malondialdehyde (MDA) assays

MDA levels were measured following the manufacturer's instructions (Beyotime, S0131S), as previously described [12]. The MDA content was calculated using a standard curve and normalized to the protein content.

2.9. Other methods

Other materials and methods were provided in Supplemental materials.

2.10. Statistical analysis

All experimental results were expressed as Mean ± standard error (Mean ± SEM), and the data were analyzed using GraphPad Prism 8.0. If the data conformed to a normal distribution, a *t*-test (two groups) or ANOVA (multiple groups) was used for analysis. If the data were not normally distributed, the Mann-Whitney *U* test (two groups) and the Kruskal-Wallis H rank-sum test (multiple groups) were used for statistical analysis. *P*-values <0.05 were used as the criterion for a significant difference.

3. Results

3.1. Hepatocytes-secreted FAM3D regulated hepatic glucose and lipid metabolism

As FAM3D is a cytokine-like molecule in humans and mice [15], serum FAM3D levels in diabetic animals and patients were analyzed. Compared to healthy subjects, serum FAM3D levels in patients with diabetes were significantly elevated (Fig. 1A) and correlated positively with fasting blood glucose levels (Fig. 1B). Serum FAM3D levels also increased in db/db- and HFD-fed mice (Fig. 1C). Consistent with a previous study [16], we observed the highest levels of FAM3D mRNA and protein expression in the mouse colon tissues (Fig. 1D-E). Significant expression of FAM3D mRNA and protein was also detected in the heart, liver, pancreas, adipose tissue, and muscles of the mice (Fig. 1D-E). FAM3D-expressing adenovirus (Ad-FAM3D) was used to infect primary mouse hepatocytes. The protein expression of FAM3D was elevated after viral infection, including both the full-length and secreted isoforms (Fig. 1F). The secreted FAM3D isoform was detected in the supernatant of primary mouse hepatocytes with or without FAM3D overexpression (Fig. 1G). These findings revealed that hepatocytes secrete FAM3D. Liver sections from control and steatotic patients were collected, and H&*E*-stained images are presented in Suppl. Fig. 1A. Immunofluorescence staining indicated that the FAM3D protein was expressed in human and mouse livers. Importantly, FAM3D expression was significantly increased in steatotic human and mouse livers (Fig. 1H-I). Subsequently, FAM3D was overexpressed in the liver of C57BL/6 J mice to evaluate its role in glucose and lipid metabolism. The body weight and glucose tolerance test data of the mice before viral injection are presented Suppl. Fig. 1B-C. Serum FAM3D levels significantly increased seven days after Ad-FAM3D injection (Fig. 1J). Hepatic FAM3D overexpression slightly improved glucose tolerance and suppressed hepatic glucose production (Fig. 1K-L). Oil Red O staining analysis revealed that liver lipid deposition was reduced after Ad-FAM3D injection (Fig. 1M), which was supported by a decrease in liver TG content (Fig. 1N). Compared with control mice, serum TG and CHO levels remained unchanged after hepatic FAM3D overexpression (Fig. 1O). Hepatic FAM3D overexpression increased the phosphorylation of Akt and FOXO1 and reduced the mRNA and protein expression of phosphoenolpyruvate carboxykinase (PEPCK) (Fig. 1P-Q). The Ad-FAM3D injection had little effect on the mRNA expression of FAM3D in the heart, pancreas, stomach, small intestine, cecum, colon, muscle, and epididymal white adipose tissue (Suppl. Fig. 1D). Accordingly, hepatocyte-secreted FAM3D may regulate hepatic glucose and lipid metabolism.

3.2. Modulation of hepatic FAM3D and FPR1 expressions on glucose and lipid metabolism in obese mice

To further probe the role of FAM3D in hepatic glucose and lipid metabolism, two groups of HFD mice with no significant differences in body weight or glucose tolerance were administered Ad-FAM3D or Ad-GFP via tail vein injection (Suppl. Fig. 1E-F). Compared to Ad-GFP-treated HFD mice, Ad-FAM3D injection significantly suppressed hepatic glucose production (Fig. 2A) and ameliorated glucose intolerance and hyperglycemia (Fig. 2B) on days three and eight post-viral injection, respectively. In another set of animals, the injection of Ad-FAM3D improved global insulin resistance in HFD mice (Fig. 2C). Morphological observations and H&E and Oil Red O staining analyses indicated that hepatic FAM3D overexpression significantly decreased liver lipid deposition (Fig. 2D-E), which was confirmed by quantitative assays of hepatic TG and CHO content (Fig. 2F). Moreover, Ad-FAM3D injection reduced serum CHO levels, but not TG levels, in HFD mice (Fig. 2G). Serum FAM3D levels (Fig. 2H) were significantly elevated after Ad-FAM3D injection, further confirming that hepatocytes secrete FAM3D. The Ad-FAM3D injection had little effect on fasting insulin levels (Suppl. Fig. 1G). Ad-FAM3D injection increased FAM3D mRNA expression in the liver (Fig. 2I), but not in the heart, pancreas, stomach, small intestine, cecum, colon, muscle, or epididymal white adipose tissues (Suppl. Fig. 1H). Hepatic FAM3D overexpression activated Akt and inactivated FOXO1, concomitant with reduced mRNA and protein expressions of glucose-6-phosphatase (G6Pase) and PEPCK in obese mouse livers (Fig. 2J-K), FAM3D has been proven to be a ligand for formyl peptide receptors (FPR1 and FPR2), and FPR is a G-protein-coupled receptor with seven transmembrane structures [22]. Therefore, we evaluated whether FAM3D regulated hepatic glucose and lipid metabolism by binding to FPRs. The transcriptional levels of FPR1 and FPR2 in the tissues of wild-type adult male C57BL/6 J mice were analyzed using quantitative PCR. Although the mRNA expression of FPR1 and FPR2 was both expressed in several tissues (Suppl. Fig. 2A-B), the mRNA level of FPR1 in the mouse liver was about 20 folds higher than that of FPR2 (Suppl. Fig. 2C), suggesting that FPR1 is the predominant FPR isoform in the liver. The protein expression of FPR1 was significantly lower in db/db mouse livers than in db/m mouse livers (Suppl. Fig. 2D). To evaluate the role of FPR1 in hepatic glucose and lipid metabolism, FPR1 was overexpressed in the livers of db/db mice using aav-FPR1. Body weight and glucose intolerance were not significantly different before tail vein injection of aav-GFP or aav-FPR1 (Suppl. Fig. 2E and Fig. 3A). The body weight of db/db mice with hepatic FPR1 overexpression began to decrease on six weeks after the viral injection (Fig. 3B). Hepatic FPR1 overexpression significantly ameliorated hyperglycemia (Fig. 3C) and

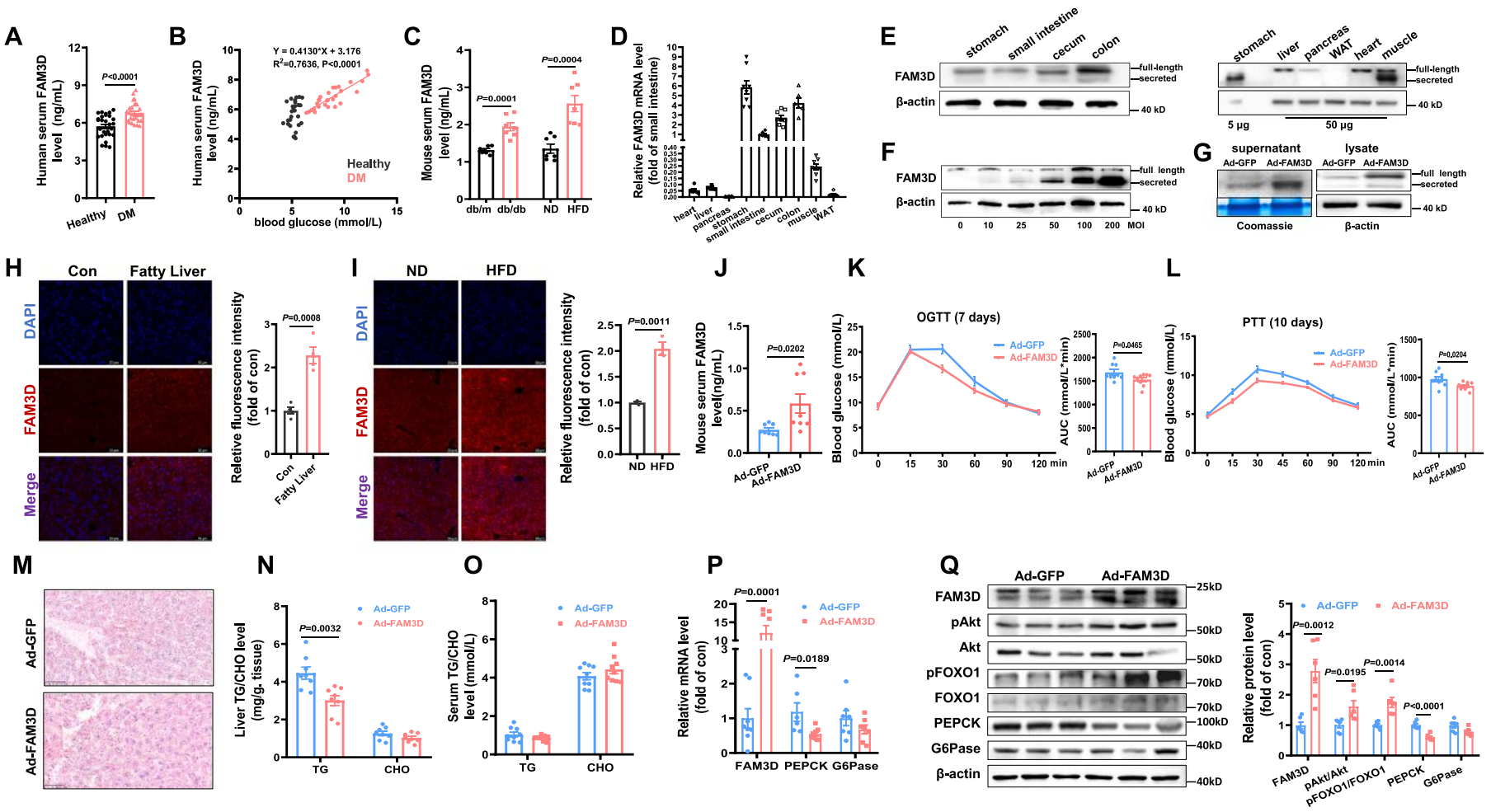

Fig. 1. Hepatocytes-secreted FAM3D regulated hepatic glucose and lipid metabolism. A) Serum FAM3D levels of patients with diabetes (DM) and healthy controls. ($n = 28$). B) The correlation between serum FAM3D level and fasting blood glucose levels in DM and healthy controls. ($n = 27$–28). C) Serum FAM3D levels was increased in db/db and high-fat diet (HFD) mice. ($n = 7$). D) Relative mRNA expressions of FAM3D across mouse tissues. E) Representative gel images of FAM3D protein expression in gastrointestinal (left) and other tissues (right); in the right panel, 5 μg stomach proteins were used as a positive control. ($n = 6$–8). F) Representative gel images of FAM3D protein expression in mouse hepatocytes infected with Ad-FAM3D or Ad-GFP. ($n = 3$). G) Representative gel images of FAM3D protein expression in the supernatant and lysate of mouse hepatocytes infected with Ad-FAM3D or Ad-GFP. Coomassie brilliant blue staining of total protein in supernatant was used as loading control. (n = 3). H) Representative immunofluorescence staining of FAM3D in the livers of NAFLD patients was shown in the left panel, and quantitative data of fluorescence intensity was shown in the right panel ($n = 4$). I) Representative immunofluorescence staining of FAM3D in HFD mouse livers are shown in the right panel, and quantitative data of fluorescence intensity is shown in the right panel. ($n = 3$). J) Serum FAM3D levels of normal C57BL/6 J mice injected with Ad-FAM3D (Ad-GFP as a control, $n = 8$). K) Oral glucose tolerance test (OGTT) on day 7 (left panel) and area under the curve (AUC) data were shown in the right panel. ($n = 9$). L) Pyruvate tolerance test (PTT) on day 10 (left panel) post adenovirus injection, and AUC data were shown in the right panel. (n = 9). M) Oil Red O staining of Ad-GFP- and Ad-FAM3D-injected mouse livers. Scale bar, 50 μm. ($n = 4$). N—O) Liver (N) and serum (O) TG and CHO levels in two groups of mice. (n = 8). P) Relative mRNA expressions of FAM3D, PEPCK, and G6Pase in the livers. (n = 7–8). Q) Hepatic FAM3D overexpression activated the Akt signaling pathway. Representative gel images of protein expression were shown in the left panel, and quantitative data was shown in the right panel. (n = 6). WAT: epididymal white adipose; ND: normal diet; MOI: multiplicity of infection; TG: serum triglyceride; CHO: cholesterol. All animals and hepatocytes were treated with Ad-GFP or Ad-FAM3D (1.5×10^9 pfu in mice, 50 MOI in cells). Statistical *P* values were labeled in each panel.

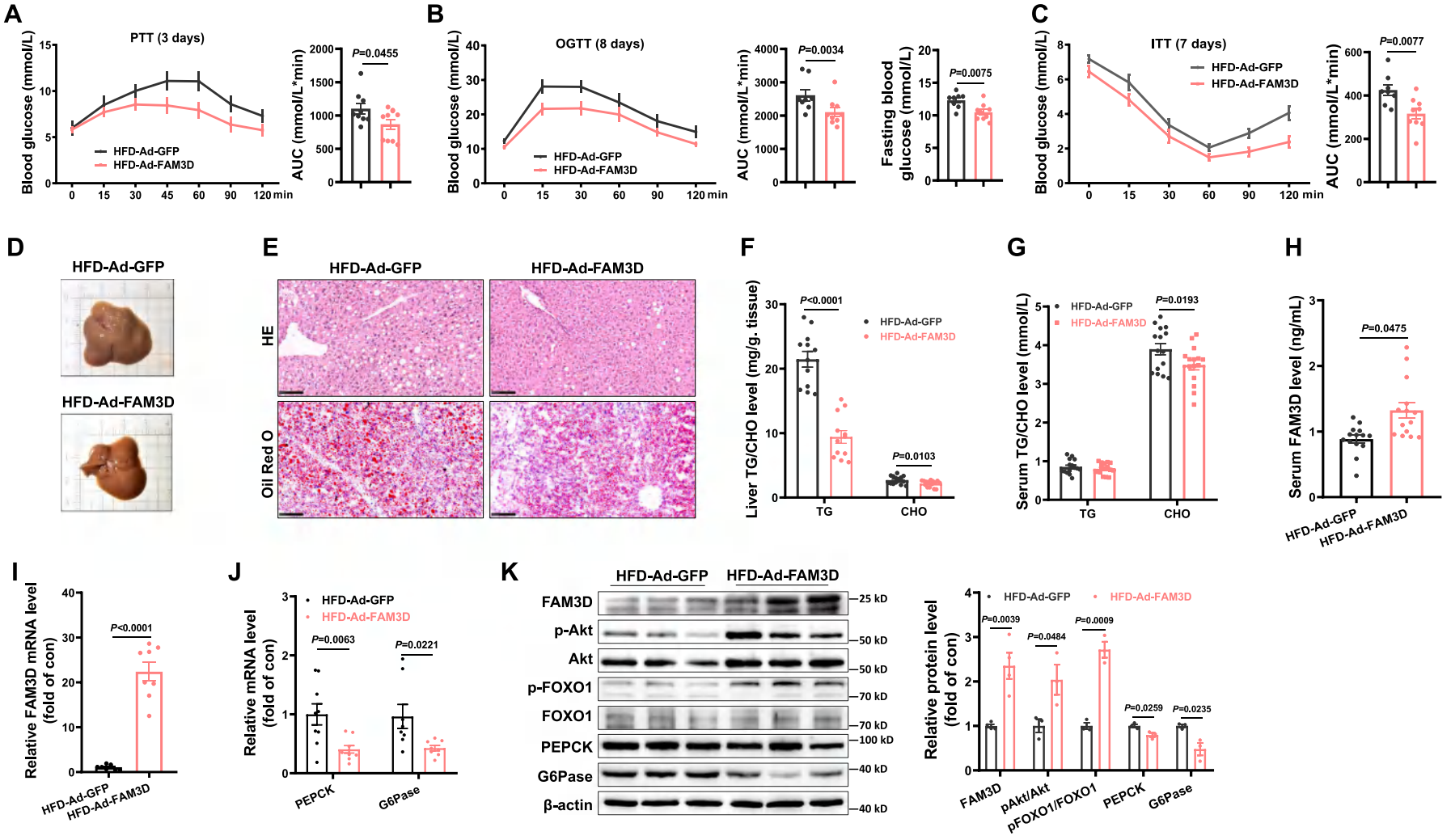

Fig. 2. Hepatic FAM3D overexpression improved dysregulated glucose and lipid metabolism in HFD mice. A) PTT on day 3 post adenoviral injection in HFD mice (left panel), and AUC data was shown in the right panel. (n = 8–9). B) OGTT on day 8 post adenoviral injection in HFD mice (left panel), AUC data was shown in the middle panel, and fasting blood glucose was shown in the right panel. (n = 8–9). C) Insulin tolerance test (ITT) on day 7 post adenoviral injection in HFD mice, and AUC data was shown in the right panel. (n = 8–9). D) Representative images of liver morphological examination in adenoviral-injected HFD mice. E) H&E (upper panel) and Oil Red O (lower panel) staining of liver tissues in adenoviral-injected HFD mice. Scale bar, 100 μm. F-G) Liver (F) and serum (G) TG/CHO content in adenoviral-injected HFD mice. (n = 12–16). H—I) Serum FAM3D level (H) and relative FAM3D mRNA expressions in livers (I) of adenoviral-injected HFD mice. (n = 8–14). J) Relative mRNA expressions of PEPCK and G6Pase in the livers of the two groups of mice (n = 8–9). K) Representative gel images of metabolic proteins in the livers of adenoviral-injected HFD mice (left panel) and quantitative data were shown in the right panel. (n = 3). All animals were treated with Ad-GFP or Ad-FAM3D (1.5×10^9 pfu). Statistical P values were labeled in each panel.

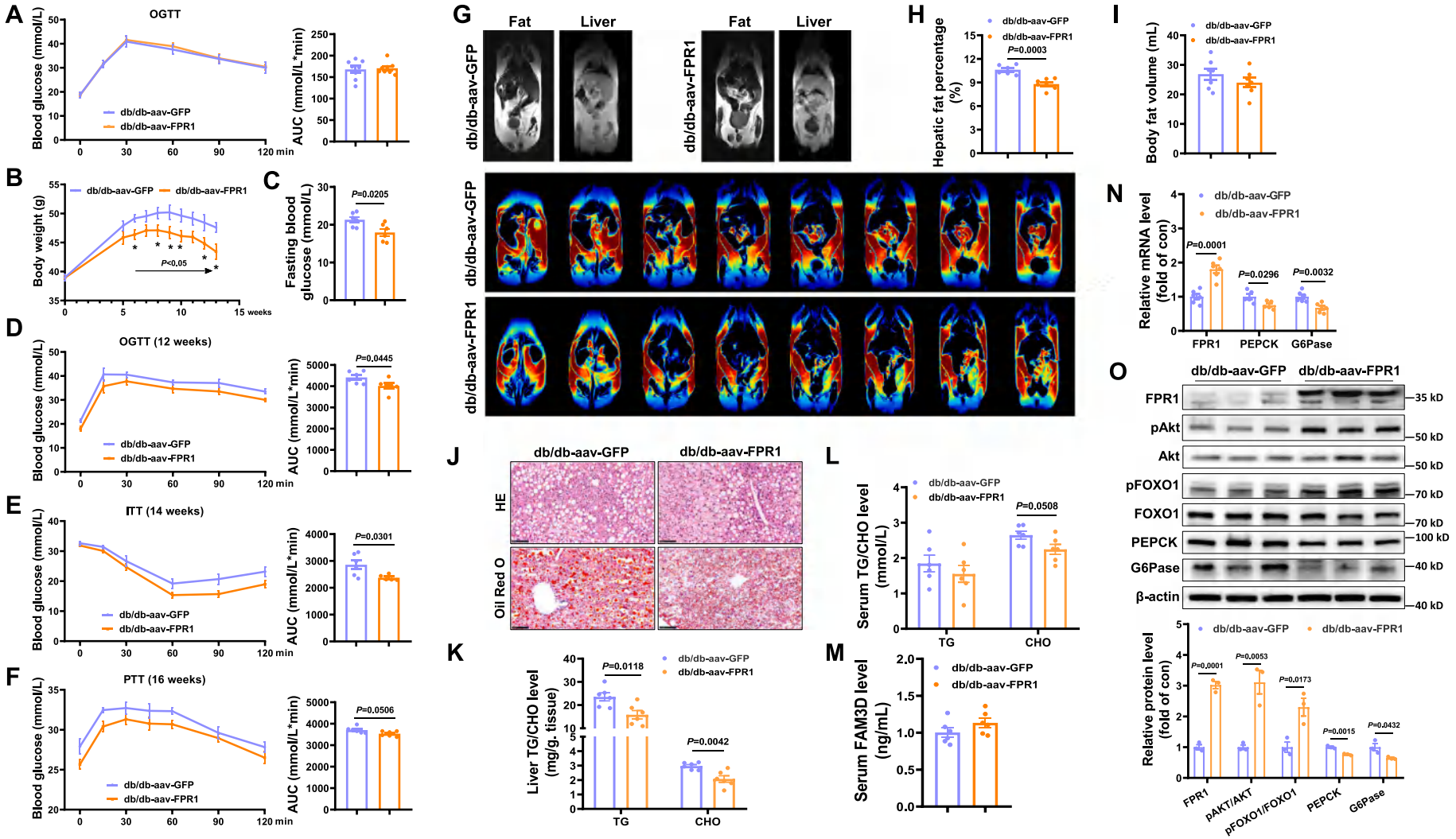

Fig. 3. Hepatic FPR1 overexpression ameliorated dysregulated glucose and lipid metabolism in db/db mice. A) OGTT in db/db mice before injection of aav-GFP or aav-FPR1. (n = 8). B) Body weight curve of db/db mice after viral injection. (n = 7–8). C) Hepatic FPR1 overexpression decreased fasting blood glucose levels on week 12 post viral injection. (n = 6). D) Hepatic FPR1 overexpression ameliorated glucose intolerance in db/db mice at 12 weeks post viral injection. OGTT data was shown in the left panel, and AUC data was shown in the right panel. E) Hepatic FPR1 overexpression enhanced global insulin sensitivity in db/db mice at 14 weeks post viral injection. ITT data was shown in left panel, and AUC data was shown in right panel. F) Hepatic FPR1 overexpression suppressed hepatic glucose production in db/db mice at 16 weeks post viral injection. PTT data was shown in the left panel, and AUC data was shown in the right panel. (n = 6). G) Representative images of whole-body fat (left) and liver fat (right) detected by MRI detection in db/db mice at 17 weeks post viral injection MRI color image analysis of fat distribution by MRI is shown in the below panel. H—I) Quantitative analyses of liver fat percentage (H) and whole-body fat content (I) in db/db mice. (n = 6). J) Representative images of H&E (upper panel) and Oil Red O staining (lower panel) of db/db mouse liver sections. Scale bar, 100 μm. K-L) Liver (K) and serum (L) TG/CHO content of db/db mice. (n = 6). M) Serum FAM3D level of db/db mice injected with viruses. (n = 6). N) Relative mRNA expressions of FPR1, PEPCK, and G6Pase in db/db mouse livers. (n = 6). O) Representative gel images of metabolic proteins in db/db mouse livers injected with viruses quantitative data were shown in the lower panel. (n = 3). All animals were treated with control (aav-GFP) or aav-FPR1 (5×10^{11} vg). Statistical *P* values were labeled in each panel. *$P < 0.05$ versus the indicated groups.

glucose intolerance (Fig. 3D), increased global insulin sensitivity (Fig. 3E), and suppressed hepatic glucose production (Fig. 3F) in db/db mice. MRI analyses revealed that aav-FPR1 injection significantly decreased hepatic fat content (Fig. 3G-H). Although there was no significant difference in total body fat volume (Fig. 3G and Fig. 3I), a reduction in body, liver, right kidney, and epididymal fat weight was observed after sacrifice (Suppl. Fig. 2F-G). Morphological observation and H&E and Oil Red O staining analyses indicated that aav-FPR1 injection decreased hepatic lipid deposition in db/db mice (Suppl. Fig. 2H-I and Fig. 3J), which was supported by quantitative assays of liver TG and CHO content (Fig. 3K). Moreover, aav-FPR1 injection reduced serum CHO but not TG levels in db/db mice (Fig. 3L). Serum FAM3D levels remained unchanged in db/db mice following hepatic FPR1 overexpression (Fig. 3M). Hepatic aav-FPR1 overexpression also activated Akt, inactivated FOXO1, and inhibited the mRNA and protein expressions of G6Pase and PEPCK in db/db mouse livers (Fig. 3N-O). aav-FPR1 injection had little effect on the mRNA expression of FPR1 in the heart, pancreas, muscle, and epididymal white adipose tissues (Suppl. Fig. 2J). Taken together, the hepatic activation of FAM3D and its receptor, FPR1, significantly ameliorated the dysregulation of glucose and lipid metabolism in obese diabetic mice.

FAM3D$^{-/-}$ mice were used to assess the role of FAM3D in glucose and lipid metabolism. The FAM3D-deficient mice are shown in Suppl. Fig. 3A. Under normal diet (ND) feeding, FAM3D$^{-/-}$ mice exhibited similar glucose tolerance and hepatic glucose production until fourteen weeks of age (Suppl. Fig. 3B-D). Therefore, another set of FAM3D-deficient mice with no differences in body weight, fasting blood glucose levels, or glucose tolerance were fed in HFD at eight weeks of age (Suppl. Fig. 3E-G). Compared to wild-type mice, the body weight (Fig. 4A) and fasting blood glucose (Fig. 4B) of FAM3D-deficient mice significantly increased after eight weeks of HFD feeding. After HFD feeding for 10–14 weeks, FAM3D-deficient mice exhibited more severe glucose intolerance, insulin resistance, and hepatic glucose production than the wild-type mice (Fig. 4C-E). Metabolic cage analyses demonstrated that the RQ, food intake, and activity were elevated, whereas EE was decreased in FAM3D-deficient mice (Fig. 4F-I). MRI analyses revealed increased body fat volume and hepatic fat percentage in FAM3D-deficient mice compared with wild-type mice (Fig. 4J-M), which was confirmed by an increase in body, heart, liver, and kidney weight after sacrifice (Suppl. Fig. 3H-I). Morphological observations and H&E and Oil Red O staining analyses revealed that FAM3D deficiency exaggerated liver lipid deposition after HFD feeding (Suppl. Fig. 3J and Fig. 4N), which was supported by the increase in hepatic TG and CHO content (Fig. 4O). Serum TG levels, but not CHO levels, increased in HFD-fed FAM3D-deficient mice (Fig. 4P). FAM3D deficiency suppressed the protein levels of pAkt and pFOXO1 and increased the mRNA and protein levels of G6Pase and PEPCK in the liver (Fig. 4Q-R). Overall, FAM3D deficiency exaggerated the dysregulation of glucose and lipid metabolism after HFD administration.

3.3. FAM3D regulated glucose and lipid metabolism by activating FPR1 in cultured hepatocytes

To determine whether the beneficial effects of FAM3D overexpression on glucose and lipid metabolism were mediated by the secreted FAM3D isoform, further experiments were performed using cultured hepatocytes. Based on the dose-dependency evaluation, 50 ng/mL recombinant FAM3D protein (rFAM3D) was used in further studies (Suppl. Fig. 3K). FAM3D overexpression significantly suppressed glucose production (Fig. 5A), promoted nuclear exclusion of FOXO1 (Fig. 5B and Suppl. Fig. 3L), and reduced lipid deposition in the presence of free fatty acids (FFAs) (Fig. 5C-D) in primary mouse hepatocytes, similar to the effects of rFAM3D treatment (Fig. 5E-H). Notably, treatment with anti-FAM3D antibodies reversed the beneficial effects of FAM3D overexpression on glucose production and lipid deposition in mouse hepatocytes (Fig. 5I-L). In support of this, FAM3D-deficient hepatocytes exhibited increased glucose production, nuclear distribution of FOXO1, lipid deposition, and TG content in the presence of FFAs compared to wild-type hepatocytes (Fig. 5M-P). These findings indicated that secretion is necessary for FAM3D's regulatory functions on glucose and lipid metabolism in hepatocytes.

To investigate whether hepatocyte-secreted FAM3D activates FPR1 to regulate glucose and lipid metabolism, primary mouse hepatocytes were infected with aav-GFP and aav-FPR1. FPR1 overexpression significantly inhibited glucose production, promoted FOXO1 nuclear exclusion, suppressed lipid deposition, and decreased TG content in primary mouse hepatocytes (Fig. 6A-D). The addition of rFAM3D further augmented the beneficial effects of FPR1 overexpression on gluconeogenesis and the repression of lipid deposition (Fig. 6A-D). In support of this, after identifying the efficiency of FPR1 siRNA in hepatocytes (Suppl. Fig. 3M), siRNA silencing of FPR1 increased glucose production and lipid deposition in primary mouse hepatocytes (Fig. 6E-H). Notably, FPR1 silencing blunted the beneficial effects of rFAM3D on gluconeogenesis and lipid deposition (Fig. 6E-H). FPR1 overexpression failed to suppress gluconeogenesis or lipid deposition in FAM3D-deficient hepatocytes (Fig. 6I-L). Importantly, the addition of rFAM3D restored the inhibitory effects of FPR1 on gluconeogenesis and lipid deposition in FAM3D-deficient hepatocytes (Fig. 6I-L). Collectively, hepatocyte-secreted FAM3D activated FPR1 to suppress glucose production and lipid deposition in hepatocytes.

3.4. FAM3D stimulates fatty acid oxidation by activating FPR1-hnRNP U-GR-SCAD pathway

To further pinpoint the mechanism(s) by which FAM3D ameliorates hepatic steatosis, high-throughput RNA sequencing was performed on primary mouse hepatocytes co-treated with aav-FPR1 and rFAM3D. The data were initially subjected to principal component analysis (PCA), and aav-FPR1- and rFAM3D-treated hepatocytes were separated from Ad-GFP control samples, indicating a distinct effect of aav-FPR1 and rFAM3D co-treatment on gene expression (Suppl. Fig. 4A). The volcano plot showed 1720 significantly altered transcripts (1424 upregulated and 296 downregulated) after aav-FPR1 plus rFAM3D treatment (Fig. 7A). Several important lipid metabolic enzymes, including lipogenesis, lipid oxidation, lipid secretion, and lipid uptake genes, were analyzed, and short-chain acyl-CoA dehydrogenase (SCAD), stearoyl-CoA desaturase 1 (SCD1), and microsomal triglyceride transfer protein (MTP1) were identified as significantly different genes after activation of the FAM3D-FPR1 axis (Fig. 7B). Moreover, these regulated genes and other known metabolic genes were analyzed using quantitative PCR assays in hepatocytes treated with Ad-FAM3D, aav-FPR1, and rFAM3D, respectively. Notably, SCAD was the only gene that was upregulated under all four conditions (Fig. 7A-E). SCAD is the key enzyme involved in lipid oxidation. Based on RNA sequencing and quantitative PCR confirmation, further studies were performed to determine whether the FAM3D-FPR1 axis upregulates SCAD to increase lipid oxidation in hepatocytes. FAM3D overexpression increased SCAD protein levels in hepatocytes (Fig. 7F). FPR1 overexpression and rFAM3D treatment also increased SCAD protein levels in hepatocytes (Fig. 7G). Moreover, FPR1 overexpression and rFAM3D treatment resulted in a stronger induction of SCAD expression than either treatment alone (Fig. 7G). Importantly, incubation with an anti-FAM3D antibody reversed the effect of FAM3D overexpression on SCAD expression in hepatocytes (Fig. 7H). In vivo, FAM3D overexpression increased, whereas FAM3D deficiency decreased, SCAD expression in the livers of HFD mice (Fig. 7I). Similarly, hepatic FPR1 overexpression also upregulated SCAD expression in the liver of db/db mice (Suppl. Fig. 4B). As SCAD is a key enzyme in lipid oxidation, the oxidation level of fatty acids was determined by measuring the malondialdehyde (MDA) level, which is a biomarker of lipid oxidation [12]. Consistent with the change in SCAD expression, lipid oxidation increased in FAM3D-overexpressed hepatocytes, which was inhibited by treatment with anti-FAM3D antibodies (Fig. 7J).

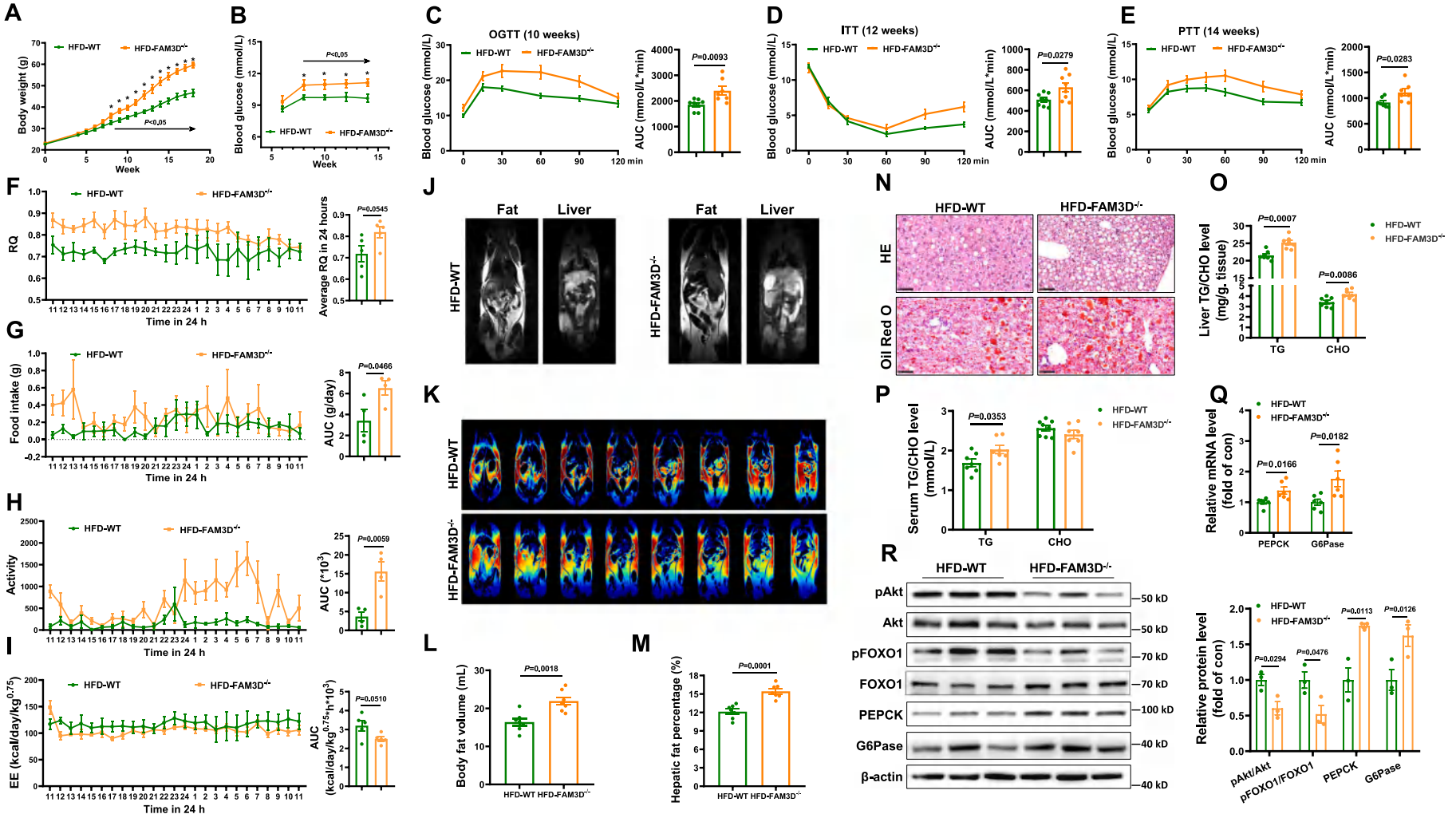

Fig. 4. FAM3D deficiency aggravated HFD-induced glucose and lipid metabolic disorders in mice. A) The weight curve of FAM3D-deficient mice (FAM3D$^{-/-}$) and wide type (WT) mice. (n = 8). B) Fasting blood glucose in mice fed on HFD. (n = 7–8). C) FAM3D deficiency aggravated HFD-induced glucose intolerance at 10 weeks. OGTT data was shown on the left panel, and AUC data was shown in the right panel. D) Increased insulin resistance in FAM3D-deficient mice after 12 weeks of HFD feeding. ITT data was shown in left panel, and AUC data was shown in the right panel. E) FAM3D deficiency aggravated HFD-induced hepatic glucose production at 14 weeks of HFD feeding. PTT data was shown in the left panel, and AUC data was in the right panel. (n = 7–8). F—I) Metabolic cage analyses of mice fed on HFD for 15 weeks. The curves of respiratory quotient (RQ) (F), food intake (G), activity (H) and energy expenditure (EE) (I) in 24 h were shown in the left penal, and the AUC data were in the right panel. (n = 4–5). J) Representative MRI images of whole-body fat (left) and liver fat (right) of mice fed on HFD 16 weeks. K) MRI color image analysis of fat distribution in the two groups of mice. L-M) Quantitative data of whole-body fat content (L) and liver fat percentage (M) in the two groups of mice. (n = 7). N) Liver sections of mice stained with H&E (upper panel) and Oil Red O (lower panel). Scale bar, 100 μm. O—P) Liver (O) and serum TG/CHO (P) levels in WT and FAM3D-deficient mice fed on HFD. (n = 7). Q) Relative mRNA expressions of PEPCK and G6Pase in two groups of mouse liver tissues. (n = 6). R) Representative gel images of metabolic proteins in the livers (left panel) and quantitative data is shown in the right panel. (n = 3). Statistical *P* values were labeled in each panel. *$P < 0.05$ versus indicated groups.

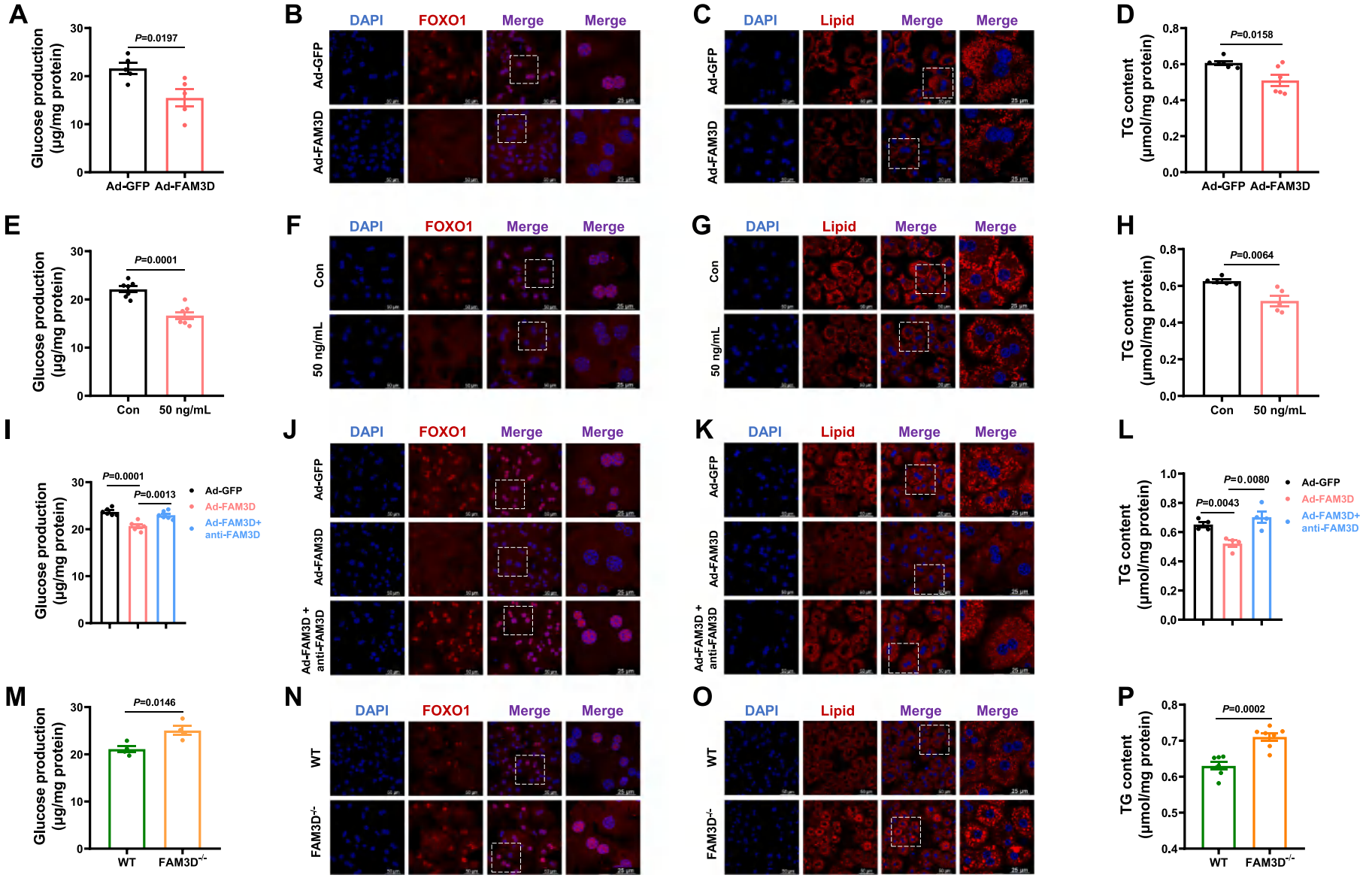

Fig. 5. Hepatocyte-secreted FAM3D inhibits gluconeogenesis and reduces lipid deposition in mouse hepatocytes. A) Glucose production level of mouse hepatocytes after Ad-FAM3D infection (50 MOI) for 24 h (Ad-GFP as a control, $n = 5$). B) Representative confocal images of FOXO1 after infection with Ad-FAM3D or Ad-GFP for 24 h. C) Representative confocal images of lipid deposition in mouse hepatocytes infected with Ad-GFP or Ad-FAM3D in the presence of free fatty acids (FFAs, 0.1 mmol/L OA + 0.2 mmol/L PA) for 24 h. D) TG content of mouse hepatocytes infected with Ad-GFP or Ad-FAM3D in the presence of FFAs. (n = 6). E) Glucose production level of mouse hepatocytes after treatment with 50 ng/mL recombinant FAM3D protein (rFAM3D) for 24 h, solvent was used as a control (Con). (n = 7). F) Representative confocal images of FOXO1 after rFAM3D or solvent (Con) treatment. G) Representative confocal images of lipid in rFAM3D-treated-mouse hepatocytes in the presence of FFAs. H) TG content in mouse hepatocytes treated with rFAM3D and Con in the presence of FFAs. (n = 5). I-L) After a 24-hour-infection of Ad-GFP or Ad-FAM3D, one group of Ad-FAM3D-treated mouse hepatocytes was treated with 2 μg/mL anti-FAM3D antibodies, and all three groups were cultured for another 12 h. I-J) Glucose production levels (I) and representative confocal images of FOXO1 in the hepatocytes (J). (n = 3–6). K-L) Representative confocal images of lipid (K) and TG content (L) in the hepatocytes in the presence of FFAs. (n = 4). M-N) Glucose production level (M) and representative confocal images of FOXO1 (N) in the FAM3D$^{-/-}$ mouse hepatocytes (WT as control, n = 4). O—P) Representative confocal images of lipid (O) and TG content (P) in FAM3D$^{-/-}$ mouse hepatocytes in the presence of FFAs. (n = 7). Statistical *P* values were labeled in each panel.

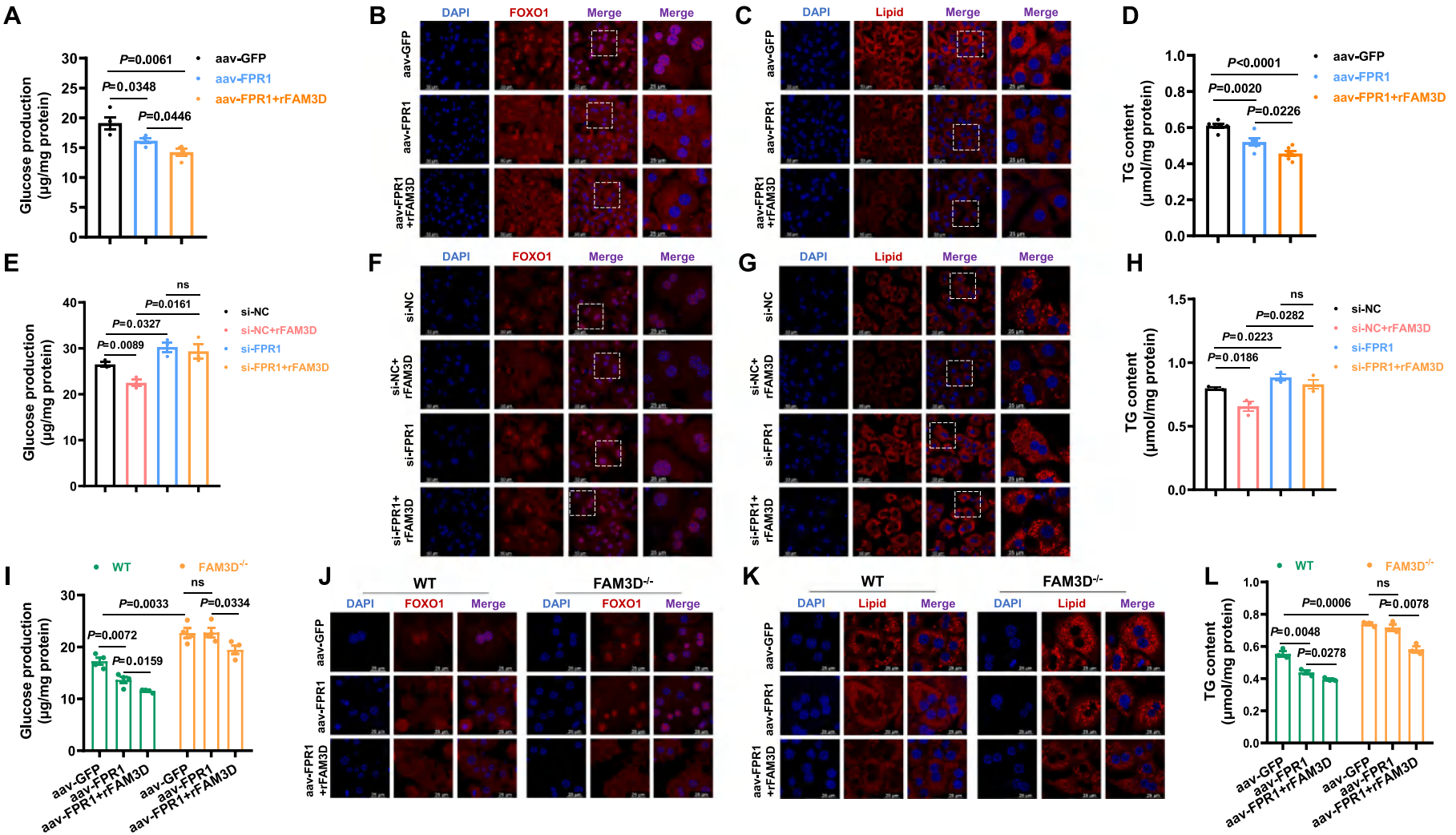

Fig. 6. FAM3D suppressed gluconeogenesis and reduced lipid deposition by activating FPR1 in mouse hepatocytes. A-D) The mouse hepatocytes were treated with 50 MOI aav-GFP (as a control), 50 MOI aav-FPR1, or 50 MOI aav-FPR1 plus 50 ng/mL rFAM3D for 36 h. Glucose production level is shown in panel A, and representative confocal images of FOXO1 shown in panel B. Representative confocal images of lipid were shown in panel C, and TG content were shown in panel D in the presence of FFAs. (n = 3–6). E-H) The mouse hepatocytes were transfected with 50 nmol/L si-NC (as a control) or 50 nmol/L si-FPR1 for 24 h with or without 50 ng/mL rFAM3D treatment. Glucose production levels (E) and representative confocal images of FOXO1 (F) in the hepatocytes. Representative confocal images of lipid (G) and TG content (H) in the hepatocytes in the presence of FFAs. (n = 3–6). I-L) The WT and FAM3D$^{-/-}$ mouse hepatocytes were administrated with 50 MOI aav-GFP (as control), 50 MOI aav-FPR1, or 50 MOI aav-FPR1 plus 50 ng/mL rFAM3D for 36 h, respectively. Glucose production level (I) and representative confocal images of FOXO1 (J) in the hepatocytes. Representative confocal images of lipid (K) and TG content (L) in the hepatocytes in the presence of FFAs. (n = 3–4). Statistical *P* values were labeled in each panel.

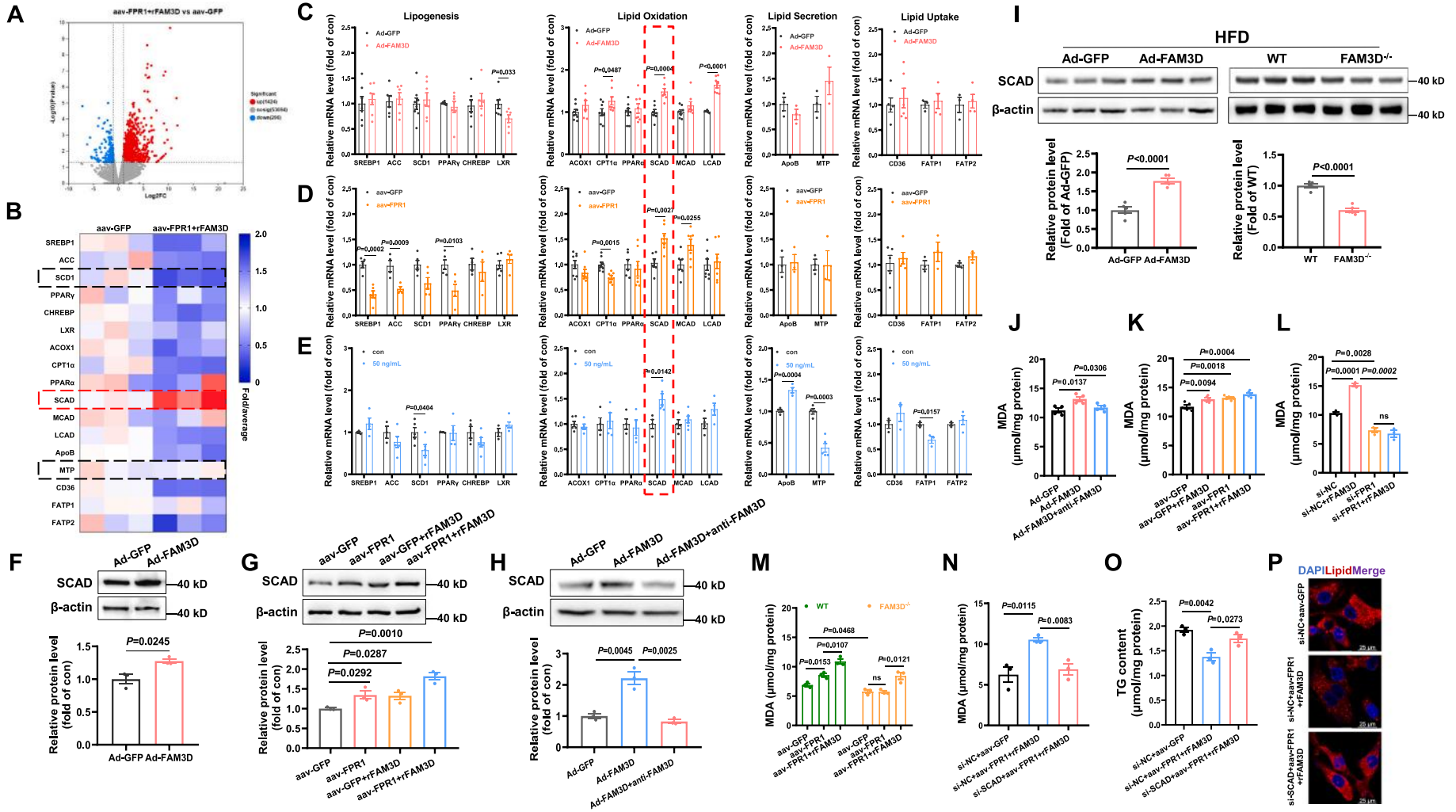

Fig. 7. FAM3D-FPR1 axis upregulated SCAD to enhance lipid oxidation in hepatocytes. A) The volcano plot of RNA-sequencing analyses of different expression genes in mouse hepatocytes infected with 50 MOI aav-GFP or 50 MOI aav-FPR1 plus 50 ng/mL rFAM3D for 36 h. (n = 3). B) Heat map of lipid metabolic genes from mouse hepatocytes treated with aav-GFP or aav-FPR1 plus rFAM3D. The color of the map represents relative expression fold changes. (n = 3). C-E) Relative expressions of typical genes in lipid metabolism, including lipogenesis, lipid oxidation, lipid secretion, and lipid uptake, from mouse hepatocytes treated with 50 MOI Ad-GFP or Ad-FAM3D (C), 50 MOI aav-GFP or aav-FPR1 (D), or 50 ng/mL rFAM3D or Con (E) for 36 h. (n = 4–8). F) FAM3D overexpression increased the protein expression of SCAD in mouse hepatocytes. Representative gel images were shown in the upper panel, and quantitative data was in the lower panel. G) Activation of the FAM3D-FPR1 axis increased SCAD in mouse hepatocytes. Representative gel images were shown in the upper panel, and quantitative data was in the lower panel. H) Anti-FAM3D antibody treatment blocked the increase of SCAD protein expression induced by FAM3D overexpression in mouse hepatocytes. Representative gel images were shown in the upper panel, and quantitative data was in the lower panel. (n = 3). I) Hepatic FAM3D overexpression increased while FAM3D deficiency decreased the protein expression of SCAD in HFD mouse livers. Representative gel images were shown in the upper panel, and quantitative data was in the below panel. (n = 5). J) Anti-FAM3D antibody treatment blunted the lipid oxidation induced by FAM3D overexpression in mouse hepatocytes in the presence of FFAs (hepatocytes treated with 50 MOI Ad-GFP, Ad-FAM3D or Ad-FAM3D plus 2 μg/mL anti-FAM3D, n = 4). K) MDA level in mouse hepatocytes treated with 50 MOI aav-FPR1 with or without 50 ng/mL rFAM3D in the presence of FFAs (aav-GFP as control, n = 5). L) MDA level in mouse hepatocytes treated with 50 nmol/L si-FPR1 with or without 50 ng/mL rFAM3D in the presence of FFAs (si-NC as control, n = 3). M) MDA level in WT and FAM3D$^{-/-}$ mouse hepatocytes treated with 50 MOI aav-FPR1 with or without 50 ng/mL rFAM3D in the presence of FFAs (aav-GFP as control, n = 3). N) MDA level in L02 cells treated with 50 nmol/L si-NC plus aav-FPR1 and rFAM3D or 50 nmol/L si-SCAD plus aav-FPR1 and rFAM3D in the presence of FFAs (aav-GFP as control, n = 3). O—P) siRNA silencing of SCAD abolished the reduction of lipid deposition induced by activation of the FAM3D-FPR1 axis in L02 cells. TG content (O) and representative confocal images of lipid (P) in L02 cells in the presence of FFAs. (n = 3). Statistical *P* values were labeled in each panel.

Oxygen-consumption rate (OCR) assay was performed to confirm whether FAM3D overexpression affects lipid oxidation. FAM3D overexpression increased the OCR and maximal respiration, which were blunted by anti-FAM3D antibodies in hepatocytes (Suppl. Fig. 4C). Furthermore, FPR1 overexpression and rFAM3D co-treatment in primary mouse hepatocytes significantly increased MDA levels (Fig. 7K). siRNA silencing of FPR1 in hepatocytes decreased lipid oxidation and maximal respiration and blunted rFAM3D-induced lipid oxidation and maximal respiration (Fig. 7L and Suppl. Fig. 4D). In FAM3D-deficient hepatocytes, lipid oxidation decreased, and FPR1 overexpression failed to increase lipid oxidation or maximal respiration (Fig. 7M and Suppl. Fig. 4E). Importantly, the administration of rFAM3D restored the ability of FPR1 overexpression to promote lipid oxidation in FAM3D-deficient hepatocytes (Fig. 7M and Suppl. Fig. 4E). To further verify that the FAM3D-FPR1 axis activates SCAD to increase lipid oxidation, SCAD expression was inhibited by siRNA transfection. The efficiency of SCAD siRNA in human hepatocytes was determined (Suppl. Fig. 4F-G). siRNA silencing of SCAD blunted the effects of FAM3D-FPR1 axis activation on promoting lipid oxidation and alleviating lipid deposition in hepatocytes (Fig. 7N-P and Suppl. Fig. 4H). Taken together, activation of the FAM3D-FPR1 axis upregulates the expression of SCAD to stimulate fatty acid oxidation, thereby ameliorating hepatic lipid deposition.

To further explore the mechanism of the FAM3D-FPR1 signaling pathway in regulating SCAD transcription, DNA pull-down was performed to identify potential transcription factors that bind to the promoter region of mouse SCAD. Three segmented DNA probe primers, covering approximately 500–700 bp of the SCAD promoter, were designed to cover the −2000 bp to +100 bp region of the mouse SCAD gene promoter. Nuclear pull-down products in mouse hepatocytes were analyzed by mass spectrometry to screen for specific transcription factors that bind to the SCAD promoter. Notably, heterogeneous nuclear ribonucleoprotein (hnRNP U) signals were detected in the pull-down products of probe 2 (−1999 bp to −1430 bp) and probe 3 (−1475 bp to −972 bp) (Fig. 8A and Suppl. Fig. 5-6). It has been reported that hnRNP U is one of the most abundant proteins in the nuclear matrix and interacts with the glucocorticoid receptor (GR) [25]. Meanwhile, our previous study showed that dexamethasone (a glucocorticoid) treatment in C57BL/6 J mice for two months significantly induced transcription of the SCAD gene in the liver using high-throughput RNA sequencing analysis [26]. In the current study, co-immunoprecipitation assays confirmed the interaction between hnRNP U and the GR in human L02 cells, which was further enhanced by aav-FPR1 and rFAM3D co-treatment (Fig. 8B). Moreover, potential binding sites for transcription factors in the promoter regions of human and mouse SCAD genes were analyzed using bioinformatic methods. Both human and mouse SCAD promoters had several potential binding sites that were highly specific for GR (Suppl. Fig. 7A). A human SCAD promoter fragment flanking −2000 bp to +100 bp, containing four predicted GR-binding sites, was synthesized and cloned into the pGL3-luciferase reporter vector plasmid. Luciferase reporter analyses indicated that GR activated the promoter activity of the human SCAD gene in L02 cells, which was further enhanced by aav-FPR1 and rFAM3D co-treatment (Fig. 8C). Furthermore, chromatin immunoprecipitation (ChIP) assays revealed that GR directly bound to the potential site (−1503 bp to -1497 bp) of the human SCAD promoter (Fig. 8D), but not to other potential sites (Suppl. Fig. 7B). Treatment with RU486, an inhibitor of GR, reversed the increase in SCAD protein expression and lipid oxidation levels and the decrease in lipid deposition in hepatocytes induced by rFAM3D and aav-FPR1 co-treatment (Fig. 8E-H and Suppl. Fig. 7C). Moreover, siRNA silencing of hnRNP U decreased the protein expression of GR and SCAD, leading to decrease lipid oxidation and increase lipid deposition in L02 cells (Fig. 8I-L). Importantly, hnRNP U inhibition blunted the beneficial effects of FAM3D-FPR1 axis activation on SCAD expression, lipid oxidation, and deposition (Fig. 8I-L).

To further investigate the mechanism of the FAM3D-FPR1 signaling pathway in regulating the interaction between hnRNP U and GR in hepatocytes, the mRNA and protein expression of GR and hnRNP U in human L02 cells were detected under FPR1 overexpression or aav-FPR1 and rFAM3D co-treatment. The mRNA and protein levels of GR and hnRNP U protein expression were increased in aav-FPR1-infected L02 cells, which was further enhanced by rFAM3D treatment (Fig. 8M-N). hnRNP U is mainly located in the nucleus [27,28], while GR is distributed in both the nucleus and cytoplasm, but mainly in the cytoplasm [29,30]. The cytoplasmic distribution of GR remained unchanged, whereas its nuclear distribution significantly increased upon activation of the FAM3D-FPR1 axis in human hepatocytes (Fig. 8O). Immunofluorescence staining showed that the nuclear distribution of GR increased in L02 cells upon activation of the FAM3D-FPR1 axis (Fig. 8P). Additionally, bioinformatic analysis revealed several potential GR binding sites in the human and mouse GR gene promoter regions (Suppl. Fig. 8). Overall, these findings reveal that activation of the FAM3D-FPR1 signaling pathway upregulates the expression of hnRNP U, which recruits the glucocorticoid receptor (GR) to the promoter region of the SCAD gene to promote its transcription, thus enhancing lipid oxidation and ameliorating lipid deposition in hepatocytes.

3.5. FAM3D-FPR1 axis suppressed hepatic gluconeogenesis via CaM-Akt pathway

The FAM3D-FPR1 axis also significantly restrained gluconeogenesis, and the underlying mechanism(s) were initially probed in cultured hepatocytes. Previous studies have demonstrated that FAM3D increases the FPR1-mediated Ca^{2+} influx into HEK293 cells [22]. We previously established that elevated intracellular Ca^{2+} concentrations activate calmodulin (CaM) to promote the phosphorylation of Akt and inhibit the expression of PEPCK and G6pase, suppressing gluconeogenesis [9]. Here, we verified that rFAM3D treatment increased intracellular Ca^{2+} influx in L02 cells, which was enhanced by FPR1 overexpression (Suppl. Fig. 9A). FAM3D overexpression increased CaM protein expression, whereas FAM3D deficiency downregulated it in the liver of HFD-fed mice (Suppl. Fig. 9B). The three CALM mRNA transcripts encode one identical CaM protein in mammals [31]. Activation of the FAM3D-FPR1 axis increased the transcription of CALM1 and CALM2 in L02 cells (Suppl. Fig. 9C). Activation of the FAM3D-FPR1 axis increased cellular CaM protein levels and pAkt levels and reduced gluconeogenic gene expression in human hepatocytes (Suppl. Fig. 9D). Treatment with CPZ, a CaM inhibitor, reversed the beneficial effects of the FAM3D-FPR1 axis on the activation of Akt, suppression of nuclear FOXO1 distribution, and gluconeogenesis in L02 cells (Suppl. Fig. 10A-C). The FAM3D-FPR1 axis activates the CaM-Akt pathway to suppress gluconeogenesis in hepatocytes.

4. Discussion

Hepatokines are designated as proteins that are secreted by hepatocytes, and hepatokines or hepatocyte-secreted proteins regulate hepatic and/or global glucose and lipid metabolism [32,33]. It has been well established that hepatokines play important roles in regulating glucose and lipid metabolism via autocrine, paracrine, and endocrine actions [32]. Clinical and experimental studies have revealed that hepatokines can exert either beneficial (sex hormone-binding globulin, fibroblast growth factor 21, angiopoietin-like protein 4, and adropin) or deleterious (α2-macroglobulin, ceruloplasmin, selenoprotein P, serotransferrin, retinol-binding protein 4, and fetuin A) metabolic effects on the liver and other tissues [32]. Although various tissues, including the pancreas, muscles, and adipose tissue, secrete fibroblast growth factor 21 (FGF-21), the main source of circulating FGF21 is the liver [34]. FGF21 has been proven to enhance insulin sensitivity, increase energy consumption, reduce body weight and serum triglyceride levels, and promote brown fat thermogenesis and fat oxidation to restore metabolic balance [35,36]. Although FGF 21 analogues in clinical trials showed no significant effects on glycemic control, they improved dyslipidemia,

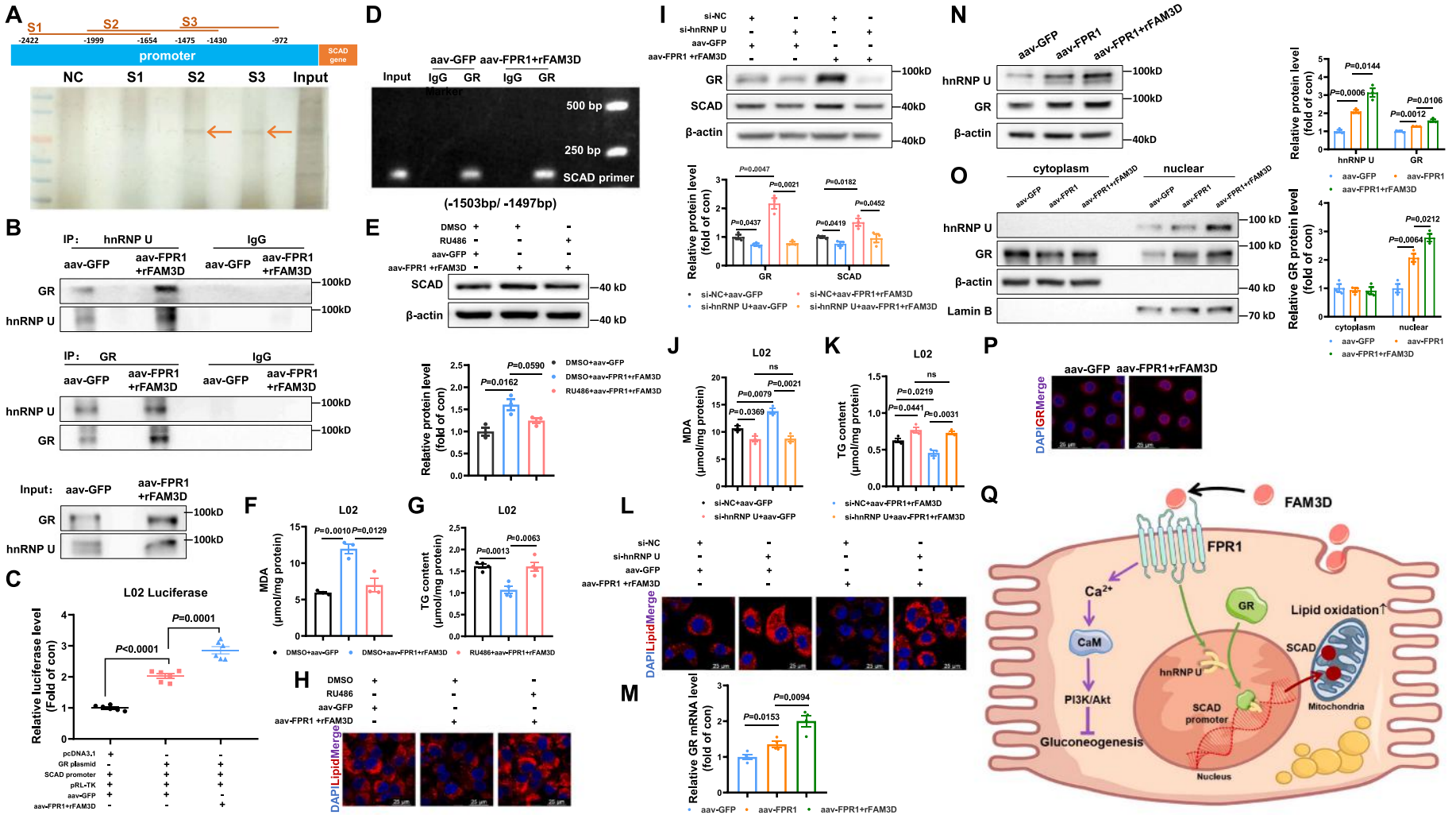

Fig. 8. FAM3D-FPR1 axis upregulated SCAD expression via enhancing the interaction between GR and hnRNP U. A) Representative silver-stained gel image of DNA pull-down products in mouse hepatocytes. The indicated bands were analyzed by mass spectrometry analysis. B) Activation of the FAM3D-FPR1 axis increased the interaction between GR and hnRNP U in L02 cells. C) A dual luciferase activity assay revealed that the human SCAD gene is a target of GR. D) Activation of the FAM3D-FPR1 axis enhanced the binding of GR to the human SCAD gene promoter in L02 cells. Representative ChIP image was shown to represent three independent experiments. E) Treatment with GR inhibitor RU486 reduced the protein expression of SCAD in L02 cells. Representative gel images were shown in upper panel, and quantitative data was shown in below panel. (n = 3). F—H) RU486 treatment reversed the increased lipid oxidation (F) and decreased lipid deposition (G-H) induced by activation of the FAM3D-FPR1 axis in the presence of FFAs in L02 cells. I) siRNA silencing hnRNP U reduced the protein expressions of GR and SCAD in L02 cells. Representative gel images were shown in the upper panel, and quantitative data was shown below. (n = 3). J-L) siRNA silencing hnRNP U reversed the increased lipid oxidation (J) and decreased lipid deposition (K-L) induced by FAM3D-FPR1 in L02 cells in the presence of FFAs. (n = 3). M) Activation of the FAM3D-FPR1 axis elevated the mRNA level of GR in L02 cells. (n = 4). N) Activation of the FAM3D-FPR1 axis increased the protein levels of hnRNP U and GR in L02 cells. Representative gel images were shown in the left panel, and quantitative data was in the right panel. (n = 3). O) Activation of FAM3D-FPR1 axis increased the nuclear distribution of hnRNP U and GR proteins in L02 cells. Representative gel images were shown in the left panel, and quantitative data was in the right panel. (n = 3). P) Representative confocal images of GR induced by activation of the FAM3D-FPR1 axis in L02 cells. Statistical *P* values were labeled in each panel. Q) Proposed model of FAM3D-FPR1 axis in the regulation of glucose and lipid metabolism. Hepatic-secreted FAM3D regulates glucose and lipid metabolism by binding to its membrane receptor, FPR1. On the one side, activation of the FAM3D-FPR1 axis increases the influx of Ca^{2+}, which activates the CaM-Akt pathway to suppress gluconeogenesis. On the other side, activation of the FAM3D-FPR1 axis upregulates the expression of hnRNP U, which recruits GR to the promoter of the SCAD gene, promoting its transcription to enhance lipid oxidation and ameliorating steatosis. Akt: protein kinase B; CaM: calmodulin; FAM3D: family with sequence similarity 3, member D; FPR1: formyl peptide receptor 1; GR: glucocorticoid receptor; hnRNP U: heterogeneous nuclear ribonucleoprotein U; PI3K: phosphoinositide 3-kinase; SCAD: short-chain acyl-CoA dehydrogenase.

hepatic lipid deposition, and fibrosis in nonalcoholic steatohepatitis (NASH) patients [37]. The development of tissue-specific delivery of FGF21 analogs may increase their therapeutic efficacy [37].

It has been previously reported that FAM3D is mainly expressed in the gut, which is regulated by nutrition status and plays critical roles in maintaining colon homeostasis [9,10,12]. In the current study, we observed that serum FAM3D levels in patients with diabetes were positively correlated with fasting blood glucose levels. We further demonstrated that FAM3D was also expressed and secreted by hepatocytes and that the expression of FAM3D was significantly increased in steatotic human and mouse livers. Ad-FAM3D injection increased the mRNA expression of FAM3D in the liver but not in other tissues, including the small intestine and colon. Serum FAM3D levels were elevated after Ad-FAM3D injection in normal and HFD mice, and Ad-FAM3D injection suppressed hepatic glucose production, ameliorated glucose intolerance, increased global insulin sensitivity, and reduced liver lipid deposition in HFD mice. Collectively, our results provide strong evidence that hepatocyte-secreted FAM3D plays an important role in the regulation of hepatic glucose and lipid metabolism.

Insulin resistance is known as the impaired insulin action in insulin-sensitive tissues, such as the liver, fat, and muscles [38]. Insulin resistance is an early stage of type 2 diabetes and is closely associated with NAFLD, NASH, obesity, and cardiovascular disease [38–40]. Dysfunction of insulin signal transduction is the main characteristic of insulin resistance [41,42]. Akt is a central node in the insulin signaling cascade [43,44]. Mice with Akt isoform deficiency exhibited insulin resistance, and patients with Akt mutations developed severe insulin resistance [45,46]. Activated Akt phosphorylates FOXO1, promotes FOXO1 translocation to the cytoplasm, and inhibits the transcription of PEPCK and G6Pase [38]. PEPCK and G6Pase are two key enzymes in hepatic gluconeogenesis, and their increased expression and activity enhance gluconeogenesis, which is highly associated with hyperglycemia [47]. An in vitro study showed that rFAM3D treatment inhibited the protein expression and activity of PEPCK and G6Pase, thus suppressing gluconeogenesis in high glucose-treated HepG2 cells [48]. This is consistent with the current study showing that FAM3D overexpression in WT and HFD-fed mice inhibited the protein expression of PEPCK and G6Pase. Mechanistically, they demonstrated that rFAM3D inhibited gluconeogenesis in a high-glucose environment via the dual specificity phosphatases 1 (DUSP1)/zinc finger protein 36 (ZFP36)/salt-induced kinase 1 (SIK1) axis [48]. Our previous studies demonstrated that both FAM3A and FAM3C activate Akt independent of insulin [9,10]. In the current study, although we did not evaluate whether the DUSP1/ZFP36/SIK1 pathway is involved in the inhibition of gluconeogenesis in FAM3D overexpressed hepatocytes, we provided strong evidence that FAM3D represses PEPCK and G6Pase expression via the CaM-Akt-FOXO1 pathway. Hepatic FAM3D overexpression increased the phosphorylation of Akt and FOXO1, and downregulated the expression of PEPCK and G6Pase in HFD-fed mouse livers. Moreover, FAM3D deficiency impairs Akt and its downstream signaling pathways, causing hepatic gluconeogenesis. In cultured hepatocytes, FAM3D overexpression and rFAM3D treatment significantly promoted FOXO1 nuclear exclusion and inhibited glucose production independent of insulin, which was blocked by anti-FAM3D antibody. Collectively, FAM3D activates Akt independent of insulin to suppress hepatic glucose production. These findings, in addition to those of our previous studies regarding FAM3A [9,11,12] and FAM3C [10], have proposed an attractive strategy for treating diabetes by activating the hepatic Akt pathway independent of insulin to suppress hepatic glucose production, which plays crucial roles in the pathogenesis of hyperglycemia, diabetes, and NAFLD.

Previous studies have revealed that insulin receptor (IR) expression in the plasma membrane is decreased in patients and mice [49–51], indicating that reduced IR levels are an important contributing factor to insulin resistance. In the current study, we observed high serum levels of FAM3D, accompanied by decreased expression of its receptor, FPR1, in diabetic mouse livers. According to the elevation of FAM3D levels in diabetic patients and mice, "FAM3D resistance" might also play important roles in the pathogenesis of diabetes and NAFLD. Subsequently, long-term hepatic FPR1 overexpression in db/db mice ameliorated glucose intolerance, increased global insulin sensitivity, suppressed hepatic glucose production, and activated Akt and downstream cascades. Previous studies have demonstrated that FAM3D increases the FPR1-mediated Ca^{2+} influx into HEK293 cells [22]. Meanwhile, elevated intracellular Ca^{2+} concentrations can activate CaM to promote Akt phosphorylation and inhibit the expression of PEPCK and G6pase, suppressing gluconeogenesis in FAM3A-overexpressed hepatocytes [9]. FAM3C overexpression in hepatocytes promotes the nuclear translocation of FOXO1 and inhibits gluconeogenesis in a CaM-dependent, but Ca^{2+}-independent manner [10]. In the current study, we found that rFAM3D treatment instantaneously increased the influx of Ca^{2+} in hepatocytes. In-depth studies have demonstrated that the FAM3D-FPR1 axis promotes the transcription of CALM1 and CALM2 to increase CaM protein expression, thus activating Akt and inhibiting PEPCK and G6Pase protein expression to suppress gluconeogenesis independent of insulin in hepatocytes. Our findings suggest that CaM is a common node molecule of the FAM3 family in glycolipid metabolism.

Previous studies revealed that reduced lipid oxidation is an important mechanism for excessive liver lipid deposition and NAFLD [52,53]. Fatty acids can be oxidized by multiple pathways, including β-oxidation, α-oxidation, and ω-oxidation [54]. In β-oxidation, long-chain fatty acids are eventually oxidized to 2 carbon units of acetyl-CoA [55]. SCAD catalyzes the oxidative dehydrogenation of 4 to 6 carbon unit length fatty acids in β-oxidation. SCAD deficiency (SCADD) is an inherited disorder characterized by the abnormal accumulation of butylcarnitine and ethylmalonic acid in the blood and urine and is clinically manifested by diverse clinical symptoms, such as severe metabolic dysfunction [56]. Misfolding of the SCAD protein increases the accumulation of reactive oxygen species (ROS), which in turn damages mitochondrial function [57]. A reduced oxygen consumption rate was observed in isolated liver mitochondria of SCAD-deficient mice. HFD-fed SCAD-deficient mice show a lower hepatic energy state [58]. In addition, mitochondrial swelling and steatosis were observed in hepatocytes isolated from another strain of SCAD-deficient mice [59]. Although dysregulated SCAD is involved in metabolic disorders, its regulatory mechanisms remain largely unknown. In the current study, we identified SCAD as a downstream gene of the FAM3D-FPR1 signaling cascade in hepatocytes. Inhibition of the FAM3D-FPR1 axis (FAM3D resistance) reduces SCAD expression, inhibits lipid oxidation, and promotes steatosis.

As is well known, GR is a ligand-dependent transcription factor that is activated by endogenous and exogenous glucocorticoids (GC). Upon activation, it is transported from the cytoplasm to the nucleus, where it regulates the transcription of target genes by binding to GC reaction elements (GRE) in the promoter regions of target genes [30,60]. Various gluconeogenic genes, such as PEPCK and G6Pase, are activated by the GC-GR signaling pathway [61]. Patients with diabetes exhibit increased plasma steroid hormone levels [62,63] and enhanced GC signaling, and GC (corticosterone) administration impairs metabolic homeostasis [60,64]. However, our previous study observed that dexamethasone treatment in C57BL/6 J mice for two months significantly induced the mRNA transcription of hepatic SCAD by high-throughput RNA sequencing analysis [26]. In addition, the current study confirmed that SCAD is a target gene of the GR. Activation of the FAM3D-FPR1 axis increases the nuclear distribution of the GR, enhances its binding to the promoter region of SCAD, and promotes its transcription. hnRNPU is one of the most abundant proteins in the nuclear matrix and interacts with GR [25]. In the current study, we demonstrated that FAM3D-FPR1 increased the interaction between the GR and hnRNP U. hnRNP-U has been reported to be a storage site for GR [65]. siRNA silencing of hnRNP U abolished the effects of FAM3D-FPR1 on increasing SCAD protein expression, promoting lipid oxidation, and suppressing lipid deposition in hepatocytes. Additionally, siRNA silencing of hnRNP U down-regulated GR protein expression. These findings indicate that the

FAM3D-FPR1 axis induces hnRNP U expression to store GR in the nucleus and supply it quickly when needed, especially to promote SCAD expression and lipid oxidation. Furthermore, the inhibition of hnRNP U might suppress the resident GR in the nucleus to restrain its transcriptional activity. The inhibition of GR using RU486 abolished the beneficial effects of FAM3D-FPR1 in promoting lipid oxidation and inhibiting lipid deposition. Collectively, in addition to the widely accepted viewpoint, the current study revealed that the GR is involved in lipid oxidation induced by the FAM3D-FPR1 axis. When the FAM3D-FPR1 axis is activated, the deleterious effect of GR on gluconeogenesis is likely blunted by the inactivation of FOXO1 and subsequent repression of gluconeogenic genes via the Ca^{2+}-CaM-Akt pathway.

In conclusion, the current study revealed that hepatocyte-released FAM3D activates the FPR1 signaling pathway to upregulate hnRNP U expression, which recruits GR to the promoter region of the SCAD gene, promoting its transcription to enhance lipid oxidation and ameliorate lipid deposition in an autocrine or paracrine manner in hepatocytes. Activating the FAM3D-FPR1 axis represents a potential strategy for the treatment of metabolic diseases, such as NAFLD and diabetes, with severe insulin resistance (Fig. 8Q).

4.1. *Significance, translational potential and limitation*

The current study has multiple great significances: 1) Hepatocyte-secreted FAM3D ameliorates hyperglycemia by activating the Ca^{2+}-CaM-Akt cascade independent of insulin to suppress hepatic gluconeogenesis. 2) Hepatocyte-secreted FAM3D activates the FPR1-hnRNP U-GR-SCAD signaling pathway to alleviate fatty liver disease by promoting lipid oxidation. 3) In contrast to the traditionally accepted deleterious effects of GR, our findings revealed a beneficial role for GR in controlling lipid oxidation in the liver. According to the vital role of hepatocyte-secreted FAM3D, promoting hepatic FAM3D secretion might be a potential therapeutic strategy for diabetes and NAFLD. Although we observed a reduction in FPR1 expression in the liver of db/db mice, suggesting the existence of FAM3D resistance in obese mice, the potential mechanism requires further exploration. Additionally, the underlying mechanism for FAM3D-FPR1 induced the transcription of hnRNP U and GR requires further clarification.

Funding

This study was supported by grants from the National Natural Science Foundation of China (82230024/82070844/82025008), the Beijing Natural Science Foundation (7212123), and the Peking University Medicine Seed Fund for Interdisciplinary Research (BMU2022PY003 and BMU2023YFJHMX002, supported by the Fundamental Research Funds for the Central Universities).

CRediT authorship contribution statement

Yuntao Hu: Conceptualization, Methodology, Data curation, Writing – original draft. **Jing Li:** Methodology, Resources, Writing – review & editing. **Xin Li:** Methodology, Data curation. **Di Wang:** Methodology, Data curation. **Rui Xiang:** Methodology. **Wenjun Liu:** Methodology. **Song Hou:** Methodology, Data curation. **Qinghe Zhao:** Methodology, Data curation. **Xiaoxing Yu:** Methodology, Resources. **Ming Xu:** Supervision, Investigation. **Dong Zhao:** Resources. **Tao Li:** Resources. **Yujing Chi:** Conceptualization, Supervision, Writing – original draft, Writing – review & editing, Project administration, Funding acquisition. **Jichun Yang:** Conceptualization, Supervision, Writing – review & editing, Project administration, Funding acquisition.

Declaration of competing interest

The authors declare that there is no conflict of interest.

Data availability

All data are available in the main text or the Supplemental materials.

Appendix A. Supplementary data

Supplementary data to this article can be found online at https://doi.org/10.1016/j.metabol.2023.155661.

References

[1] Younossi ZM, Koenig AB, Abdelatif D, Fazel Y, Henry L, Wymer M. Global epidemiology of nonalcoholic fatty liver disease-Meta-analytic assessment of prevalence, incidence, and outcomes. Hepatology 2016;64:73–84. https://doi.org/10.1002/hep.28431.
[2] Allen AM, Lazarus JV, Younossi ZM. Healthcare and socioeconomic costs of NAFLD: a global framework to navigate the uncertainties. J Hepatol 2023. https://doi.org/10.1016/j.jhep.2023.01.026.
[3] Younossi ZM, Golabi P, Paik JM, Henry A, Van Dongen C, Henry L. The global epidemiology of nonalcoholic fatty liver disease (NAFLD) and nonalcoholic steatohepatitis (NASH): a systematic review. Hepatology 2023;77:1335–47. https://doi.org/10.1097/HEP.0000000000000004.
[4] Estes C, Anstee QM, Arias-Loste MT, Bantel H, Bellentani S, Caballeria J, et al. Modeling NAFLD disease burden in China, France, Germany, Italy, Japan, Spain, United Kingdom, and United States for the period 2016-2030. J Hepatol 2018;69:896–904. https://doi.org/10.1016/j.jhep.2018.05.036.
[5] Polyzos SA, Kountouras J, Mantzoros CS. Obesity and nonalcoholic fatty liver disease: From pathophysiology to therapeutics. Metabolism 2019;92:82–97. https://doi.org/10.1016/j.metabol.2018.11.014.
[6] Papadopoulos G, Legaki AI, Georgila K, Vorkas P, Giannousi E, Stamatakis G, et al. Integrated omics analysis for characterization of the contribution of high fructose corn syrup to non-alcoholic fatty liver disease in obesity. Metabolism 2023;144:155552. https://doi.org/10.1016/j.metabol.2023.155552.
[7] Zhang X, Yang W, Wang J, Meng Y, Guan Y, Yang J. FAM3 gene family: A promising therapeutical target for NAFLD and type 2 diabetes. Metabolism 2018;81:71–82. https://doi.org/10.1016/j.metabol.2017.12.001.
[8] Li J, Chi Y, Wang C, Wu J, Yang H, Zhang D, et al. Pancreatic-derived factor promotes lipogenesis in the mouse liver: role of the Forkhead box 1 signaling pathway. Hepatology 2011;53:1906–16. https://doi.org/10.1002/hep.24295.
[9] Wang C, Chi Y, Li J, Miao Y, Li S, Su W, et al. FAM3A activates PI3K p110alpha/Akt signaling to ameliorate hepatic gluconeogenesis and lipogenesis. Hepatology 2014;59:1779–90. https://doi.org/10.1002/hep.26945.
[10] Chen Z, Ding L, Yang W, Wang J, Chen L, Chang Y, et al. Hepatic activation of the FAM3C-HSF1-CaM pathway attenuates hyperglycemia of obese diabetic mice. Diabetes 2017;66:1185–97. https://doi.org/10.2337/db16-0993.
[11] Yan H, Meng Y, Li X, Xiang R, Hou S, Wang J, et al. FAM3A maintains metabolic homeostasis by interacting with F1-ATP synthase to regulate the activity and assembly of ATP synthase. Metabolism 2023;139:155372. https://doi.org/10.1016/j.metabol.2022.155372.
[12] Liu X, Hou S, Xiang R, Hu C, Chen Z, Li N, et al. Imipramine activates FAM3A-FOXA2-CPT2 pathway to ameliorate hepatic steatosis. Metabolism 2022;136:155292. https://doi.org/10.1016/j.metabol.2022.155292.
[13] Chi Y, Meng Y, Wang J, Yang W, Wu Z, Li M, et al. FAM3B (PANDER) functions as a co-activator of FOXO1 to promote gluconeogenesis in hepatocytes. J Cell Mol Med 2019;23:1746–58. https://doi.org/10.1111/jcmm.14073.
[14] Chen Z, Liu X, Luo Y, Wang J, Meng Y, Sun L, et al. Repurposing doxepin to ameliorate steatosis and hyperglycemia by activating FAM3A signaling pathway. Diabetes 2020;69:1126–39. https://doi.org/10.2337/db19-1038.
[15] de Wit NJW, IJssennagger N, Oosterink E, Keshtkar S, Hooiveld GJEJ, Mensink RP, et al. Oit1/Fam3D, a gut-secreted protein displaying nutritional status-dependent regulation. J Nutr Biochem 2012;23:1425–33. https://doi.org/10.1016/j.jnutbio.2011.09.003.
[16] Liang W, Peng X, Li Q, Wang P, Lv P, Song Q, et al. FAM3D is essential for colon homeostasis and host defense against inflammation associated carcinogenesis. Nat Commun 2020;11:5912. https://doi.org/10.1038/s41467-020-19691-z.
[17] Johansson ME, Phillipson M, Petersson J, Velcich A, Holm L, Hansson GC. The inner of the two Muc2 mucin-dependent mucus layers in colon is devoid of bacteria. Proc Natl Acad Sci U S A 2008;105:15064–9. https://doi.org/10.1073/pnas.0803124105.
[18] de Wit NJ, Bosch-Vermeulen H, de Groot PJ, Hooiveld GJ, Bromhaar MM, Jansen J, et al. The role of the small intestine in the development of dietary fat-induced obesity and insulin resistance in C57BL/6J mice. BMC Med Genet 2008;1:14. https://doi.org/10.1186/1755-8794-1-14.
[19] Cao T, Yang D, Zhang X, Wang Y, Qiao Z, Gao L, et al. FAM3D inhibits glucagon secretion via MKP1-dependent suppression of ERK1/2 signaling. Cell Biol Toxicol 2017;33:457–66. https://doi.org/10.1007/s10565-017-9387-8.
[20] Tanowitz M, Von Zastrow M. Ubiquitination-independent trafficking of G protein-coupled receptors to lysosomes. J Biol Chem 2002;277:50219–22. https://doi.org/10.1074/jbc.C200536200.
[21] He HQ, Ye RD. The formyl peptide receptors: diversity of ligands and mechanism for recognition. Molecules 2017:22. https://doi.org/10.3390/molecules22030455.

[22] Peng X, Xu E, Liang W, Pei X, Chen D, Zheng D, et al. Identification of FAM3D as a new endogenous chemotaxis agonist for the formyl peptide receptors. J Cell Sci 2016;129:1831–42. https://doi.org/10.1242/jcs.183053.
[23] He L, Fu Y, Deng J, Shen Y, Wang Y, Yu F, et al. Deficiency of FAM3D (Family With sequence similarity 3, Member D), a novel chemokine, attenuates neutrophil recruitment and ameliorates abdominal aortic aneurysm development. Arterioscler Thromb Vasc Biol 2018;38:1616–31. https://doi.org/10.1161/ATVBAHA.118.311289.
[24] Prossnitz ER, Quehenberger O, Cochrane CG, Ye RD. Transmembrane signalling by the N-formyl peptide receptor in stably transfected fibroblasts. Biochem Biophys Res Commun 1991;179:471–6. https://doi.org/10.1016/0006-291x(91)91394-r.
[25] Eggert M, Michel J, Schneider S, Bornfleth H, Baniahmad A, Fackelmayer FO, et al. The glucocorticoid receptor is associated with the RNA-binding nuclear matrix protein hnRNP U. J Biol Chem 1997;272:28471–8. https://doi.org/10.1074/jbc.272.45.28471.
[26] Cui A, Fan H, Zhang Y, Zhang Y, Niu D, Liu S, et al. Dexamethasone-induced Kruppel-like factor 9 expression promotes hepatic gluconeogenesis and hyperglycemia. J Clin Invest 2019;129:2266–78. https://doi.org/10.1172/JCI66062.
[27] Geuens T, Bouhy D, Timmerman V. The hnRNP family: insights into their role in health and disease. Hum Genet 2016;135:851–67. https://doi.org/10.1007/s00439-016-1683-5.
[28] Han SP, Tang YH, Smith R. Functional diversity of the hnRNPs: past, present and perspectives. Biochem J 2010;430:379–92. https://doi.org/10.1042/BJ20100396.
[29] Heitzer MD, Wolf IM, Sanchez ER, Witchel SF, DeFranco DB. Glucocorticoid receptor physiology. Rev Endocr Metab Disord 2007;8:321–30. https://doi.org/10.1007/s11154-007-9059-8.
[30] Gulliver LS. Xenobiotics and the glucocorticoid receptor. Toxicol Appl Pharmacol 2017;319:69–79. https://doi.org/10.1016/j.taap.2017.02.003.
[31] Nojima H, Sokabe H. Structural organization of calmodulin genes in the rat genome. Adv Exp Med Biol 1989;255:223–32. https://doi.org/10.1007/978-1-4684-5679-0_24.
[32] Meex RCR, Watt MJ. Hepatokines: linking nonalcoholic fatty liver disease and insulin resistance. Nat Rev Endocrinol 2017;13:509–20. https://doi.org/10.1038/nrendo.2017.56.
[33] Namkung J, Koh SB, Kong ID, Choi JW, Yeh BI. Serum levels of angiopoietin-related growth factor are increased in metabolic syndrome. Metabolism 2011;60:564–8. https://doi.org/10.1016/j.metabol.2010.05.013.
[34] Markan KR, Naber MC, Ameka MK, Anderegg MD, Mangelsdorf DJ, Kliewer SA, et al. Circulating FGF21 is liver derived and enhances glucose uptake during refeeding and overfeeding. Diabetes 2014;63:4057–63. https://doi.org/10.2337/db14-0595.
[35] Camporez JP, Jornayvaz FR, Petersen MC, Pesta D, Guigni BA, Serr J, et al. Cellular mechanisms by which FGF21 improves insulin sensitivity in male mice. Endocrinology 2013;154:3099–109. https://doi.org/10.1210/en.2013-1191.
[36] Gong Q, Hu Z, Zhang F, Cui A, Chen X, Jiang H, et al. Fibroblast growth factor 21 improves hepatic insulin sensitivity by inhibiting mammalian target of rapamycin complex 1 in mice. Hepatology 2016;64:425–38. https://doi.org/10.1002/hep.28523.
[37] Geng L, Lam KSL, Xu A. The therapeutic potential of FGF21 in metabolic diseases: from bench to clinic. Nat Rev Endocrinol 2020;16:654–67. https://doi.org/10.1038/s41574-020-0386-0.
[38] Saltiel AR. Insulin signaling in health and disease. J Clin Invest 2021:131. https://doi.org/10.1172/JCI142241.
[39] Czech MP. Insulin action and resistance in obesity and type 2 diabetes. Nat Med 2017;23:804–14. https://doi.org/10.1038/nm.4350.
[40] Lee WH, Najjar SM, Kahn CR, Hinds Jr TD. Hepatic insulin receptor: new views on the mechanisms of liver disease. Metabolism 2023;145:155607. https://doi.org/10.1016/j.metabol.2023.155607.
[41] Yaribeygi H, Farrokhi FR, Butler AE, Sahebkar A. Insulin resistance: Review of the underlying molecular mechanisms. J Cell Physiol 2019;234:8152–61. https://doi.org/10.1002/jcp.27603.
[42] Khalid M, Alkaabi J, Khan MAB, Adem A. Insulin signal transduction perturbations in insulin resistance. Int J Mol Sci 2021:22. https://doi.org/10.3390/ijms22168590.
[43] Manning BD, Cantley LC. AKT/PKB signaling: navigating downstream. Cell 2007;129:1261–74. https://doi.org/10.1016/j.cell.2007.06.009.
[44] Du F, Liu M, Wang J, Hu L, Zeng D, Zhou S, et al. Metformin coordinates with mesenchymal cells to promote VEGF-mediated angiogenesis in diabetic wound healing through Akt/mTOR activation. Metabolism 2023;140:155398. https://doi.org/10.1016/j.metabol.2023.155398.
[45] Cho H, Mu J, Kim JK, Thorvaldsen JL, Chu Q, Crenshaw 3rd EB, et al. Insulin resistance and a diabetes mellitus-like syndrome in mice lacking the protein kinase Akt2 (PKB beta). Science 2001;292:1728–31. https://doi.org/10.1126/science.292.5522.1728.
[46] George S, Rochford JJ, Wolfrum C, Gray SL, Schinner S, Wilson JC, et al. A family with severe insulin resistance and diabetes due to a mutation in AKT2. Science 2004;304:1325–8. https://doi.org/10.1126/science.1096706.
[47] Petersen MC, Vatner DF, Shulman GI. Regulation of hepatic glucose metabolism in health and disease. Nat Rev Endocrinol 2017;13:572–87. https://doi.org/10.1038/nrendo.2017.80.
[48] Huang B, Luo YL, Huang JL, Li GZ, Qiu SY, Huang CC. FAM3D inhibits gluconeogenesis in high glucose environment via DUSP1/ZFP36/SIK1 axis. Kaohsiung J Med Sci 2023;39:254–65. https://doi.org/10.1002/kjm2.12633.
[49] Soll AH, Kahn CR, Neville Jr DM. Insulin binding to liver plasm membranes in the obese hyperglycemic (ob/ob) mouse. Demonstration of a decreased number of functionally normal receptors. J Biol Chem 1975;250:4702–7.
[50] Caro JF, Ittoop O, Pories WJ, Meelheim D, Flickinger EG, Thomas F, et al. Studies on the mechanism of insulin resistance in the liver from humans with noninsulin-dependent diabetes. Insulin action and binding in isolated hepatocytes, insulin receptor structure, and kinase activity. J Clin Invest 1986;78:249–58. https://doi.org/10.1172/JCI112558.
[51] Choi E, Kikuchi S, Gao H, Brodzik K, Nassour I, Yopp A, et al. Mitotic regulators and the SHP2-MAPK pathway promote IR endocytosis and feedback regulation of insulin signaling. Nat Commun 2019;10:1473. https://doi.org/10.1038/s41467-019-09318-3.
[52] Puri P, Baillie RA, Wiest MM, Mirshahi F, Choudhury J, Cheung O, et al. A lipidomic analysis of nonalcoholic fatty liver disease. Hepatology 2007;46:1081–90. https://doi.org/10.1002/hep.21763.
[53] Xu T, Lim YT, Chen L, Zhao H, Low JH, Xia Y, et al. A novel mechanism of monoethylhexyl phthalate in lipid accumulation via inhibiting fatty acid beta-oxidation on hepatic cells. Environ Sci Technol 2020;54:15925–34. https://doi.org/10.1021/acs.est.0c01073.
[54] Du X, Osoro EK, Chen Q, Yan X, Gao D, Wu L, et al. Pdcd4 promotes lipid deposition by attenuating PPARalpha-mediated fatty acid oxidation in hepatocytes. Mol Cell Endocrinol 2022;545:111562. https://doi.org/10.1016/j.mce.2022.111562.
[55] Bartlett K, Eaton S. Mitochondrial beta-oxidation. Eur J Biochem 2004;271:462–9. https://doi.org/10.1046/j.1432-1033.2003.03947.x.
[56] Nochi Z, Olsen RKJ, Gregersen N. Short-chain acyl-CoA dehydrogenase deficiency: from gene to cell pathology and possible disease mechanisms. J Inherit Metab Dis 2017;40:641–55. https://doi.org/10.1007/s10545-017-0047-1.
[57] Schmidt SP, Corydon TJ, Pedersen CB, Bross P, Gregersen N. Misfolding of short-chain acyl-CoA dehydrogenase leads to mitochondrial fission and oxidative stress. Mol Genet Metab 2010;100:155–62. https://doi.org/10.1016/j.ymgme.2010.03.009.
[58] Ghosh S, Kruger C, Wicks S, Simon J, Kumar KG, Johnson WD, et al. Short chain acyl-CoA dehydrogenase deficiency and short-term high-fat diet perturb mitochondrial energy metabolism and transcriptional control of lipid-handling in liver. Nutr Metab (Lond) 2016;13:17. https://doi.org/10.1186/s12986-016-0075-0.
[59] Armstrong DL, Masiowski ML, Wood PA. Pathologic characterization of short-chain acyl-CoA dehydrogenase deficiency in BALB/cByJ mice. Am J Med Genet 1993;47:884–92. https://doi.org/10.1002/ajmg.1320470616.
[60] Wu T, Shao Y, Li X, Wu T, Yu L, Liang J, et al. NR3C1/Glucocorticoid receptor activation promotes pancreatic beta-cell autophagy overload in response to glucolipotoxicity. Autophagy 2023:1–20. https://doi.org/10.1080/15548627.2023.2200625.
[61] Chen G, Wang R, Chen H, Wu L, Ge RS, Wang Y. Gossypol ameliorates liver fibrosis in diabetic rats induced by high-fat diet and streptozocin. Life Sci 2016;149:58–64. https://doi.org/10.1016/j.lfs.2016.02.044.
[62] Hollenberg NK, Stevanovic R, Agarwal A, Lansang MC, Price DA, Laffel LM, et al. Plasma aldosterone concentration in the patient with diabetes mellitus. Kidney Int 2004;65:1435–9. https://doi.org/10.1111/j.1523-1755.2004.00524.x.
[63] Hofmann A, Peitzsch M, Brunssen C, Mittag J, Jannasch A, Frenzel A, et al. Elevated steroid hormone production in the db/db mouse model of obesity and Type 2 diabetes. Horm Metab Res 2017;49:43–9. https://doi.org/10.1055/s-0042-116157.
[64] D'Souza AM, Beaudry JL, Szigiato AA, Trumble SJ, Snook LA, Bonen A, et al. Consumption of a high-fat diet rapidly exacerbates the development of fatty liver disease that occurs with chronically elevated glucocorticoids. Am J Physiol Gastrointest Liver Physiol 2012;302:G850–63. https://doi.org/10.1152/ajpgi.00378.2011.
[65] Eggert H, Schulz M, Fackelmayer FO, Renkawitz R, Eggert M. Effects of the heterogeneous nuclear ribonucleoprotein U (hnRNP U/SAF-A) on glucocorticoid-dependent transcription in vivo. J Steroid Biochem Mol Biol 2001;78:59–65. https://doi.org/10.1016/s0960-0760(01)00074-7.